Tran-SET

Transportation Consortium of South-Central States

Solving Emerging Transportation Resiliency, Sustainability, and Economic Challenges through the Use of Innovative Materials and Construction Methods: From Research to Implementation

Mitigating Reflective Cracking Through the Use of a Ductile Concrete Interlayer

Project No. 18PLSU13

Lead University: University of Louisiana at Lafayette

Final Report

September 2019

Disclaimer

The contents of this report reflect the views of the authors, who are responsible for the facts and the accuracy of the information presented herein. This document is disseminated in the interest of information exchange. The report is funded, partially or entirely, by a grant from the U.S. Department of Transportation's University Transportation Centers Program. However, the U.S. Government assumes no liability for the contents or use thereof.

Acknowledgements

The authors would like to acknowledge the support by the Transportation Consortium of South-Central States (Tran-SET).

TECHNICAL DOCUMENTATION PAGE

1. Project No.	2. Government Accession No.	3. Recipient's Catalog No.
18PLSU13		

4. Title and Subtitle	5. Report Date
Mitigating Reflective Cracking Through the Use of a Ductile Concrete Interlayer	Sept. 2019
	6. Performing Organization Code
7. Author(s)	**8. Performing Organization Report No.**
PI: Qian Zhang https://orcid.org/0000-0001-8142-1533 Co-PI: Mohammad J.Khattak https://orcid.org/0000-0003-2780-4909 GRA: Adway Das https://orcid.org/0000-0001-8246-7242	
9. Performing Organization Name and Address	**10. Work Unit No. (TRAIS)**
Transportation Consortium of South-Central States (Tran-SET) University Transportation Center for Region 6 3319 Patrick F. Taylor Hall, Louisiana State University, Baton Rouge, LA 70803	**11. Contract or Grant No.** 69A3551747106
12. Sponsoring Agency Name and Address	**13. Type of Report and Period Covered**
United States of America Department of Transportation Research and Innovative Technology Administration	Final Research Report Mar. 2018 – Mar. 2019
	14. Sponsoring Agency Code

15. Supplementary Notes

Report uploaded and accessible at Tran-SET's website (http://transet.lsu.edu/).

16. Abstract

Reflective cracking is considered one of the most important issues that causes premature deterioration of composite pavements. Many types of mitigation methods have been studied in the past. However, they are either not effective in delaying the reflective cracking, or they only extend the service life by a few years. To address this critical issue and significantly extend the service life of the composite pavement, in this research, a ductile interlayer made of engineered cementitious composites (ECC) was proposed. It was hypothesized that by adding a thin layer of highly ductile ECC material between the existing pavement and overlay, reflective cracking could be arrested by the ductile interlayer. This study experimentally evaluated the effectiveness of ECC as an interlayer system. A laboratory test protocol was designed to simulate repeated traffic loads to measure the fatigue performance of ECC interlayer system. The strain field and reflective cracking were monitored using digital image correlation (DIC) technique. It was found that the composite pavement specimens with ECC interlayer provided significantly higher fatigue life as compared to the control specimens without an interlayer. The failure mode also changed from single reflective crack to multiple cracks in overlaid HMA mixtures. The results indicated that ECC could be used as a potential effective interlayer system to retard or mitigate reflective cracking.

17. Key Words	18. Distribution Statement
ECC, Interlayer, Reflective Cracks, Overlay, Pavement	No restrictions. This document is available through the National Technical Information Service, Springfield, VA 22161.

19. Security Classif. (of this report)	20. Security Classif. (of this page)	21. No. of Pages	22. Price
Unclassified	Unclassified	37	

Form DOT F 1700.7 (8-72) **Reproduction of completed page authorized.**

SI* (MODERN METRIC) CONVERSION FACTORS

APPROXIMATE CONVERSIONS TO SI UNITS

Symbol	When You Know	Multiply By	To Find	Symbol
		LENGTH		
in	inches	25.4	millimeters	mm
ft	feet	0.305	meters	m
yd	yards	0.914	meters	m
mi	miles	1.61	kilometers	km
		AREA		
in^2	square inches	645.2	square millimeters	mm^2
ft^2	square feet	0.093	square meters	m^2
yd^2	square yard	0.836	square meters	m^2
ac	acres	0.405	hectares	ha
mi^2	square miles	2.59	square kilometers	km^2
		VOLUME		
fl oz	fluid ounces	29.57	milliliters	mL
gal	gallons	3.785	liters	L
ft^3	cubic feet	0.028	cubic meters	m^3
yd^3	cubic yards	0.765	cubic meters	m^3
		NOTE: volumes greater than 1000 L shall be shown in m^3		
		MASS		
oz	ounces	28.35	grams	g
lb	pounds	0.454	kilograms	kg
T	short tons (2000 lb)	0.907	megagrams (or "metric ton")	Mg (or "t")
		TEMPERATURE (exact degrees)		
^oF	Fahrenheit	5 (F-32)/9 or (F-32)/1.8	Celsius	^oC
		ILLUMINATION		
fc	foot-candles	10.76	lux	lx
fl	foot-Lamberts	3.426	$candela/m^2$	cd/m^2
		FORCE and PRESSURE or STRESS		
lbf	poundforce	4.45	newtons	N
lbf/in^2	poundforce per square inch	6.89	kilopascals	kPa

APPROXIMATE CONVERSIONS FROM SI UNITS

Symbol	When You Know	Multiply By	To Find	Symbol
		LENGTH		
mm	millimeters	0.039	inches	in
m	meters	3.28	feet	ft
m	meters	1.09	yards	yd
km	kilometers	0.621	miles	mi
		AREA		
mm^2	square millimeters	0.0016	square inches	in^2
m^2	square meters	10.764	square feet	ft^2
m^2	square meters	1.195	square yards	yd^2
ha	hectares	2.47	acres	ac
km^2	square kilometers	0.386	square miles	mi^2
		VOLUME		
mL	milliliters	0.034	fluid ounces	fl oz
L	liters	0.264	gallons	gal
m^3	cubic meters	35.314	cubic feet	ft^3
m^3	cubic meters	1.307	cubic yards	yd^3
		MASS		
g	grams	0.035	ounces	oz
kg	kilograms	2.202	pounds	lb
Mg (or "t")	megagrams (or "metric ton")	1.103	short tons (2000 lb)	T
		TEMPERATURE (exact degrees)		
^oC	Celsius	1.8C+32	Fahrenheit	^oF
		ILLUMINATION		
lx	lux	0.0929	foot-candles	fc
cd/m^2	$candela/m^2$	0.2919	foot-Lamberts	fl
		FORCE and PRESSURE or STRESS		
N	newtons	0.225	poundforce	lbf
kPa	kilopascals	0.145	poundforce per square inch	lbf/in^2

TABLE OF CONTENTS

LIST OF FIGURES

LIST OF TABLES

ACRONYMS, ABBREVIATIONS, AND SYMBOLS

AADT	Annual Average Daily Traffic
AASHTO	American Association of State Highway and Transportation Officials
ADT	Average Daily Traffic
APT	Accelerated Pavement Testing
CIR	Cold-In-place Recycling
CRCP	Continuously Reinforced Concrete Pavement
CRM	Crumb-Rubber Modifier
CTR	Construction Time Ratio
DGAC	Dense-Grade Asphalt Overlay
DRM	Distress Resistant Membrane
ECC	Engineered Cementitious Composite
ESAL	Equivalent Single Axle Load
FE	Finite Element
FEA	Finite Element Analysis
FHWA	Federal Highway Administration
HMA	Hot Mix Asphalt
HPFRC	High Performance Fiber Reinforced Concrete
IRF	International Road Federation
IRI	International Roughness Index
LADOTD	Louisiana Department of Transportation and Development
LCCA	Life-Cycle Cost Analysis
LTRC	Louisiana Transportation Research Center
MCR	Material Cost Ratio
NCAT	National Center for Asphalt Technology
PCC	Portland Cement Concrete
PCI	Pavement Condition Index
PVC	Poly Vinyl Chloride
SAMI	Stress Absorbing Membrane Interlayer

USDOT	United States Department of Transportation

EXECUTIVE SUMMARY

Reflective cracking is considered one of the most important issues that cause premature deterioration of composite pavements. Many types of mitigation methods have been studied in the past. However, they are either not effective in delaying the reflective cracking, or they only extend the service life by a few years. To address this critical issue and significantly extend the service life of the composite pavement, in this research, a ductile interlayer made of engineered cementitious composites (ECC) was proposed. It was hypothesized that by adding a thin layer of highly ductile ECC material between the existing pavement and overlay, reflective cracking could be arrested by the ductile interlayer and this hypothesis was experimentally evaluated in this research project.

In this project, world-wide literature were reviewed to identify the current practice of pavement overlay systems; currently used interlayer systems and design and their limitations; available ECC mixtures and properties; and testing methods and standards for pavement interlayers and overlays. This information was used to facilitate the design and testing of the proposed ECC interlayers.

A laboratory test protocol was designed. Small scale specimens with and without ECC interlayers were prepared and tested under three-point flexural fatigue loadings to simulate repeated traffic loadings. The fatigue life of the specimens was then determined based on the testing data and used to evaluate the effectiveness of the ECC interlayer system.

The major findings of this research are listed below:

- Existing methods to prevent or retard reflective cracking include polymer modification of asphalt mixtures, saw, and seal, rigid interlayers like galvanized steel net, geogrids, and softer interlayers like Geosynthetics, SAMI, membranes, and composites. However, these treatments either have their own drawbacks or only extend the service life by a few years and therefore did not fully solve the problem of reflective cracking.
- ECC interlayer significantly delays reflective crack growth by providing a firm base underneath the HMA. It was found that thicker ECC interlayer (12.5 mm) increased fatigue life by 140% while the thinner ECC interlayer (6.5 mm) showed 70% improvement under point load.
- Test results also illustrated that the ECC interlayer distributes the stress concentration at the joint to a broader area. For fatigue test, ECC reduced the tensile stress level on the bottom of HMA, which delayed reflective crack initiation, propagation, and acceleration. This delay ultimately increased the fatigue life of the ECC specimen. Instead of one single reflective crack as observed in the control specimen, ECC interlayer specimen under point load generated multiple reflective cracks, which were merged together at failure. But in case of distributed load, ECC interlayer specimen cracks were generated at the top of the HMA and propagated downward.
- ECC interlayer beam did not show any significant strain and crack during ramp loading and fatigue tests. It was observed that the crack initiated and propagated through the HMA only.

The results of the experimentation clearly indicate that ECC has high potential to be used as an interlayer system to mitigate reflective cracking in composite pavements.

1. INTRODUCTION

Overlays are constructed over existing pavement structures as a repair measure. When an overlay is placed on the existing pavement, under thermal, shrinkage or traffic induced loadings, cracking of the overlay often takes place at locations where there are joints or cracks in the underlying pavement due to stress concentration. This phenomenon is referred to as reflective cracking. Reflective cracking in the overlay allows water to penetrate the pavement structure and contributes to many forms of pavement deterioration, including increased roughness, spalling, and decreased fatigue life *(1)*. Therefore, to achieve an effective and durable pavement repair using the overlay system, reflective cracking needs to be suppressed.

In the past, researchers have investigated various methods to mitigate the problems of reflective cracking, including saw and seal, fractured slabs, and many forms of interlayers. However, the majority of the methods are either not effective or only extend the service of the pavement overlay by a few years. A new method to suppress or significant delay reflective cracking is in desperate need.

In this research, a ductile Engineered Cementitious Composite (ECC) which is a high-performance fiber reinforced concrete (HPFRC) interlayer, was proposed in this research to mitigate the reflective cracking problem in pavement overlays. It was hypothesized that by adding a thin layer of highly ductile ECC material between the existing pavement and overlay, reflective cracking could be arrested by the ductile interlayer.

ECC is a special kind of fiber reinforced concrete that exhibits strain hardening behavior and high ductility under tension *(2-4)*. Unlike conventional brittle concrete, ECC forms multiple tight cracks under tension before the final fracture, which leads to high deformation capacity and fracture resistance. Studies also showed that using ECC as overlays for the repair of the bridge deck and rigid pavement successfully suppressed reflective cracking and dramatically extended the fatigue life of the repair *(5-12)*. Although ECC overlays have been demonstrated to be effective, constructing the entire overlay using ECC is costly. Therefore, in this research, an ECC interlayer was proposed.

In the proposed interlayer system, a thin precast layer of ECC was placed between the existing pavement and the actual overlay. The performance of the proposed ECC interlayer was experimentally evaluated in this study.

2. OBJECTIVES

This research assessed the performance of the proposed innovative interlayer system. The new repair system is expected to have much higher structural and durability performance than that of the currently used overlay and interlayer system. The overall objective of the project is to design and evaluate the behavior and fatigue performance of a novel interlayer (ECC) system made of ductile ECC. The specific objectives are:

- Review the current practice of pavement interlayer system.
- Experimentally study the performance of the proposed ECC interlayer system.
- Make design recommendations of ECC interlayer system.
- Disseminate the research findings through various educational and outreach programs

The scope of this project includes the following specific tasks that were completed to achieve the project objective.

2.1. Task 1: Review of Worldwide Literature

The literature review was conducted to identify:

- The current practice of pavement overlay systems
- Currently used interlayer systems and design and their limitations.
- Available ECC mixtures and properties.
- Testing methods and standards for pavement interlayers and overlays.

2.2. Task 2-3: Experimentation

In the experimental program, a recently developed ECC mixture using locally accessible sand and fibers were selected, and its mechanical properties were characterized. Lab scale specimens similar to that shown in Figure 1 were prepared and tested under static and cyclic three-point flexural loadings. The measured fatigue behavior and fatigue life of samples with ECC interlayer and control specimens (without interlayers) were compared to evaluate the effectiveness of the ECC interlayer to suppress the reflective cracking and to find the optimal design of the ECC interlayer system.

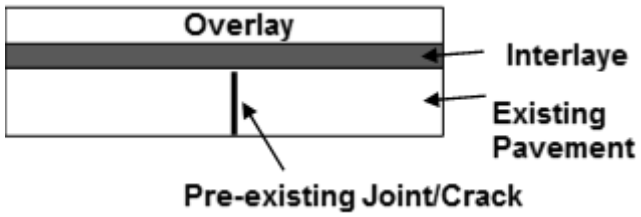

Figure 1. Interlayer specimen configuration.

2.3. Task 4-5: Data Analysis and Reporting

Analysis of all experimental data obtained from the above tasks was conducted. The performance of the proposed interlayer system was evaluated based on all experimental data. All the findings of test results, data analysis, and conclusions are documented in this report.

3. LITERATURE REVIEW

3.1. Introduction

Hot Mix Asphalt (HMA) overlays are constructed over existing pavement structures as a repair measure. When HMA is overlaid over an existing Portland Cement Concrete (PCC) layer, tensile stress concentrates at the bottom of the HMA at the location of transverse joints or pre-cracks in the PCC underlayer. After a certain period, this tensile stress generates micro cracks at the maximum strain origination area due to this tensile stress. Eventually, the microcracks transformed into macrocracks and propagate to the surface of the HMA overlay. This phenomenon is known as Reflective Cracking (see Figure 2).

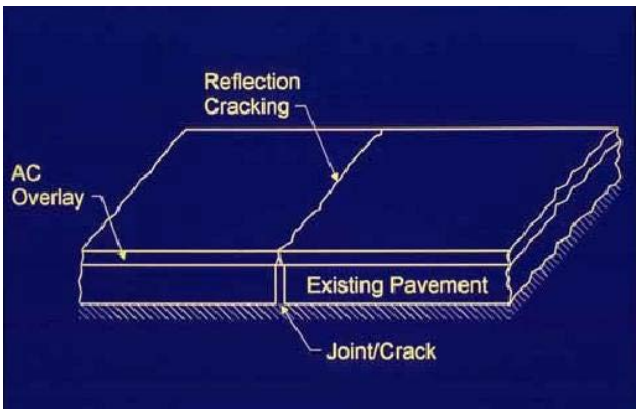

Figure 2. Propagation of reflective crack from the existing concrete pavement into the new asphalt overlay *(13)*.

Reflective cracking in the overlay allows water to penetrate the pavement structure and contributes to many forms of pavement deterioration, including increased roughness, spalling, and decreased fatigue life. According to a survey data, (see Figure 3) *(1)* collected from 25 states, the Quebec Department of Transportation, and the Saskatchewan Ministry of Highway and Infrastructure (Canada), the average service life of a 1.5–2.0 inch. (38.1–50.8 mm) HMA overlay against reflection cracking is just 1 to 6 years.

Figure 3. The average service life of an HMA overlay against reflection cracking *(1)*.

3.2. Mechanism of Reflective Cracking

Reflective cracks propagate to the pavement surface at an average rate of approximately 1 inch per year, and within around three years, it appears in the surface *(2)*. The propagation of the Reflective cracking can be divided into two different stages, that are crack initiation at the bottom of the overlay stage and crack propagation to the top surface of the overlay stage. The reflective cracks in an overlay can be formed because of two reasons. One is due to thermal loading which is in generally introduced to HMA overlay for the horizontal and vertical movement of the underlying rigid pavement due to temperature variation, and another one is traffic induced loading (see Figure 4). Traffic-induced loading may have more contribution than thermal loading in the origination of reflective crack, but the thermal load plays the significant role in propagating the crack from the bottom of the overlay to the surface *(1)*. Also, in a survey, It was also noticed that the states with a short service life of HMA (1–3 years) are mainly located in the northern region of the US and Canada. This trend is expected due to the impacts of thermal movement on the fast propagation of reflection cracking *(1)*. According to Lytton et al. *(4)*, the traffic induced load over a crack in the existing pavement causes three critical pulses (one maximum bending and two maximum shear stresses).

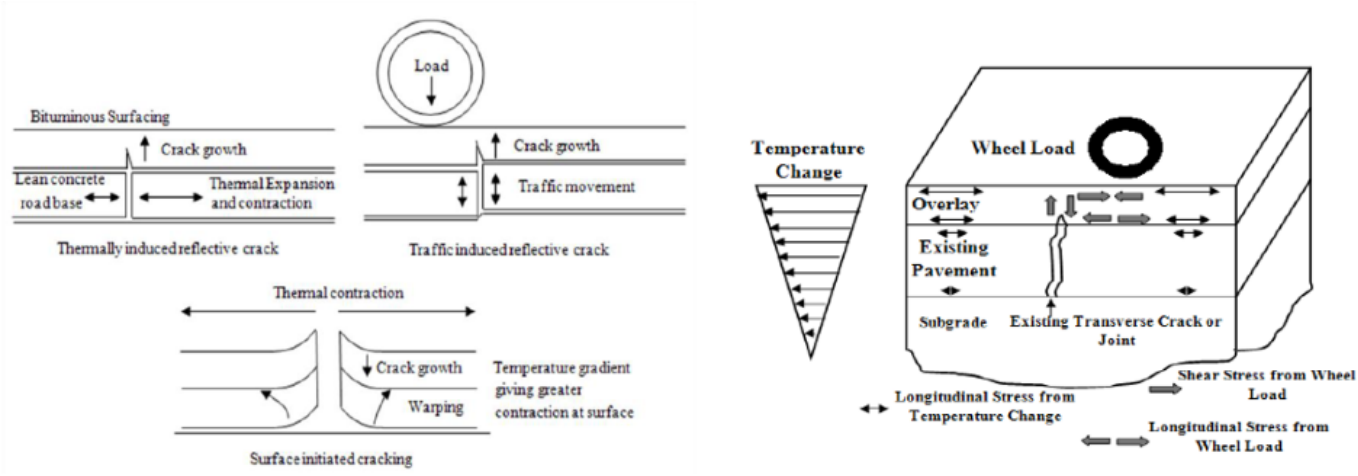

Figure 4. Mechanism of reflective cracking due to two different kinds of loading *(5)*.

3.3. Different Modes of Loading Responsible For Reflective Cracking

Generally, these two types of loads are applied on a pavement structure as a combination of three different modes (see Figure 5), which represent the worst cases of loading for fracture *(5)*: Mode 1: loads normally applied to the crack plane (thermal and traffic loading); Mode 2: In-plane shear loading, which leads to crack faces sliding against each other normal to the leading edge of the crack (traffic loading); and Mode 3: Out-of-plane shear loading parallel to the crack leading edge. This mode of loading is known as tearing mode, but the real effect of this mode in reflective crack formation in the composite pavement is questionable.

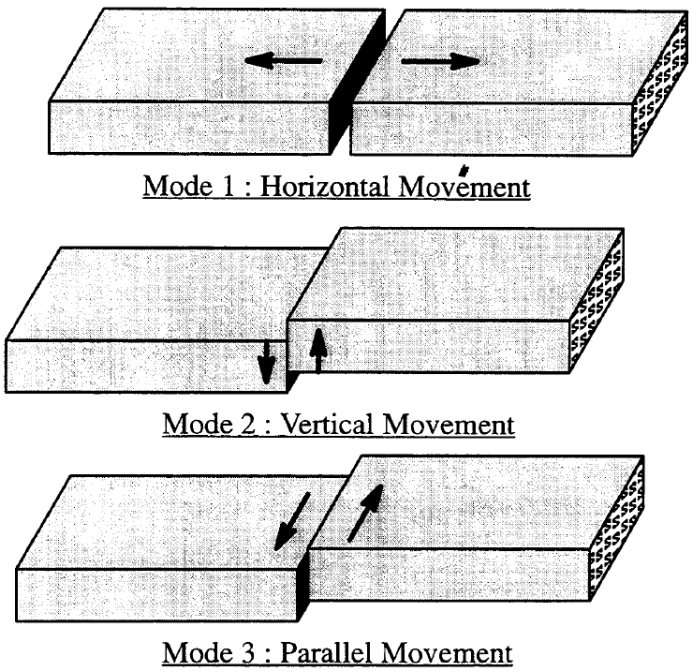

Figure 5. Different modes of fracture *(5)*.

3.4. Current Practice of Overlay System

In the current highway systems in the United States, there are about 850,000 lane km of Portland Cement Concrete (PCC) or rigid pavements, where at least 50 percent of them are Interstate system *(14)*. Any deterioration of the highway systems can adversely affect the road users' safety, vehicle operating costs, ride quality, and the cost of highway maintenance. To overcome the situation, Hot mix asphalt overlay has been recognized as a viable solution of rigid pavement rehabilitation. Asphalt overlays are not only used to improve the functional behavior of an already distressed rigid pavement, but it can also be used to reduce the noise, increase the skid resistivity, and improvement of the ride quality. Asphalt overlays can be placed over pavements in various degrees of distress, and the performance of the overlay depends upon the preparation of the existing pavement. The most beneficial aspect of asphalt overlay is the cost-effectiveness of this rehabilitating method for an existing roadway. Another significant benefit of the asphalt overlay is construction speed and convenience. AC overlays can be constructed on flexible or rigid pavement without significant traffic obstruction or redirection. Nevertheless, the use of the overlay rather than costlier alternatives (e.g., full-depth repair), is another benefit. Whereas expensive options can provide the required structural serviceability, often a major rehabilitation which involves a simple AC overlay of the proper thickness can save both time and money. Another benefit of asphalt overlay is the versatility, which can be applied either as a maintenance technique to eradicate unexpected environmental or traffic loading or as a rehabilitation process to increase the service life of an existing pavement.

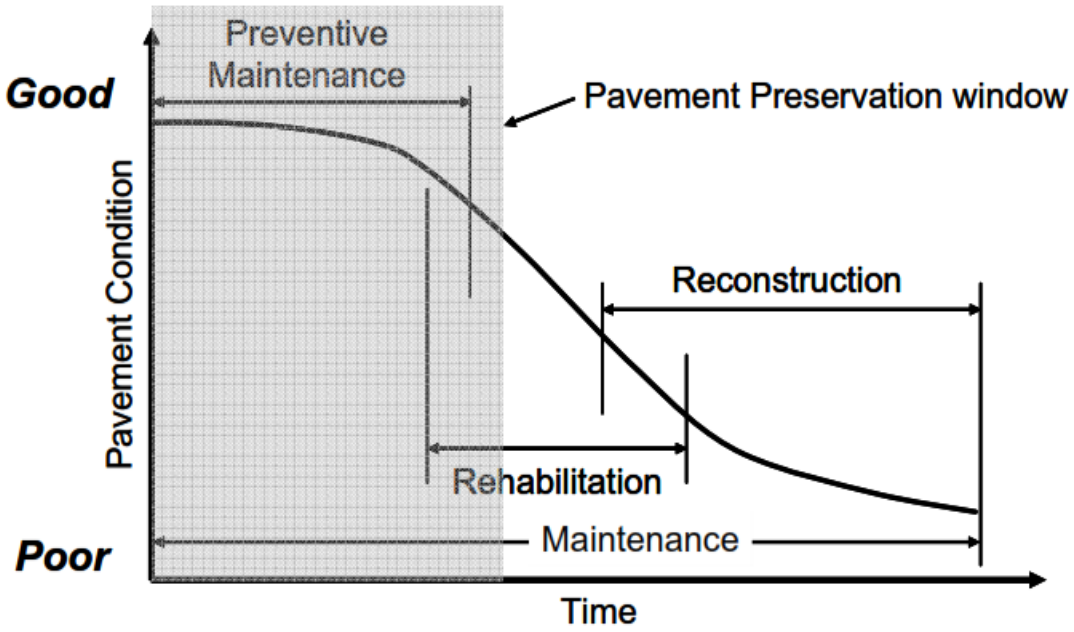

Figure 6. Terms for pavement improvement efforts relative to condition of pavement over time *(15)*.

3.4.1. Changes in The HMA Overlay Design

The researchers used a different technique to reduce the reflective by using more adaptable asphalts modified with polymer or rubber or changing the depth of the asphalt overlay for an increment of the design life against reflective cracking.

Increasing the HMA Overlay Thickness: Finn et al. developed the empirical relation between the thickness of HMA and minimization of reflective cracking from local experiences *(16)*. The type of pavement (HMA or PCC), nature of distresses, environmental conditions, and traffic loadings were the main parameter of that empirical relation. Later, many researchers had updated the findings of the relationships between reflective cracking and HMA overlay thickness:

- In Georgia, Gulden et al. had found that the 20% area of cracking for a 6-inch overlay takes around six years while it is just two years for a 4-inch overlay on PCC pavement. A 2-inch overlay showed almost no resistance against reflective cracking *(17)*.
- Predoehl et al. researched in California, which showed that 4.8 inches of the overlay could reduce reflective cracking for ten years. With the prerequisite condition that the old pavement is structurally sound and adequately repaired *(18)*.
- McLaughlin et al. investigated reflective cracking in the airport pavements and experienced severe reflective cracking when a thin overlay (about 2 inches) is placed over pre-cracked HMA or PCC pavement. This research showed that a 4-inch overlay could arrest reflective cracking better than the previously used thinner overlay *(19)*.

Special Type of Design in Overlay: The bituminous mix design is modified by the addition of synthetic fibers (polypropylene or polyester), ground scrap tire rubber, and geosynthetic materials. The above technique increases the overlay's tensile strength or flexibility (compliance), which helps in minimizing reflective cracking without disturbing the stability of the overlay. But sometimes, the use of harder asphalts may increase the tensile strength in the overlay, but due to lower flexibility will cause other types of crackings in the pavement such as rutting or flushing.

The balance between increasing the tensile strength and maintaining proper flexibility is the fundamental objective of modified HMA design:

- McLaughlin et al. *(19)* used a crumb rubber HMA overlay at the Phoenix International Airport and other pavements in Arizona, which showed high performance in fatigue cracking and reflective crack resistance.
- Button et al. performed a series of laboratory and field tests with eight types of chopped synthetic fibers as an additive in HMA overlays. This investigation indicated that in a laboratory test of fabrics mixed in asphalt concrete specimens improved the tensile properties, increased fatigue performance, and reduced crack propagation rate, and compound overlay slippage problems can be eliminated, but that operation requires better field compaction of the overlay *(20)*.
- Beckham et al. constructed eight experimental sections using cotton fabric to reinforce HMA surface treatments on both roads and wooden bridge floors between 1926 and 1935 in South Carolina and achieved superior durability *(21)*.
- Lytton et al. described three uses of geotextiles: reinforcing, strain relief, and undersealing in their report. They made a systematic approach to test the fracture properties of the HMA overlay for crack growth prediction. This research provides design equations for determining the thickness of HMA overlay. The major problem with designing an overlay system with geosynthetic is the lack of product characteristics information except some index properties provided by the manufacturers which are not crucial for pavement design *(4)*.

3.4.2. Different Pre-Overlay Concrete Pavement Repair and Preparation

While constructing asphalt overlay on an existing PCC pavement, it is recommended that all the discontinuities and distresses in the rigid pavement, like deteriorated joints, cracks, and punchouts must be corrected with full-depth repairs before the overlaying process. It helps in reducing reflective cracking. In this surface preparation process, strong bonding between two layers can be achieved through one or a combination of the following methods *(22)*:

- Texturing the PCC surface;
- Cleaning the PCC surface; and
- Placing the proper type and quantity of tack coat on the cleaned PCC surface.

The asphalt overlay can correct specific distress in the pavement by itself and restore ride quality, but It is important to eliminate the causes of different distresses from the original concrete pavement before overlay. But it cannot fix problems such as loss of support, poor drainage, full depth cracks, or low load transfer between slabs. Failure to resolve these issues before overlaying will reduce the effectiveness of the asphalt overlay. Once all repairs have been made, the surface of the concrete slab needs to be cleaned and prepared to start the overlaying. Small particles are removed from the surface by sweeping or compressed air. *(23)*. For areas with hard to remove substances like mud, water spraying may be used for cleaning, but the portion must be dry before the application of the overlay.

Fractured Slab Techniques for Preparing PCC Underlayer: As an alternative to traditional pre-overlay repairs, the existing concrete pavement can be repaired by breaking it into many pieces to create a base layer on which the asphalt overlay can be placed. “Crack-and-seating” and “Rubblization” are two types of fractured slab techniques that can be used as a reflective crack

mitigation process in asphalt overlays of concrete pavements. These techniques are useful for deteriorated rigid pavements *(24)*.

Crack and Seat: In this technique, the slab is cracked into roughly two feet in diameter pieces, and a roller is used for seating the broken pieces, which helps to create a firm and relatively leveled base for the asphalt overlay. Load transfer is partially preserved between the slab-lets, but the potential for reflective cracking is reduced. Seating re-establishes contact and support between the concrete slab and the underlying layers which have been lost in the deterioration period. Possible weak areas in the base or subgrade can be located during the rolling process and must be replaced before the overlay is placed *(25)*.

Rubblization: This process is similar to crack-and-seat, except that the resulting concrete pieces are 2-3 inches at the surface of the PCC layer. Rubblizing destroys the integrity of the slab, and can't transfer load between the pieces *(26)*, and it is not considered as a suitable pre-overlay treatment for pavements with poor subgrade support *(27)*. After rubblization, the pavement must be rolled before the overlaying, which is similar to seating cracked pavement in the crack-and-seat procedure. It is used to create a solid, stable base to overlay the asphalt concrete. In both methods, the existing concrete slab is crushed into small pieces (see Figure 7) before placement of the overlay. The difference between the two processes is the size of the resulting pieces of concrete. The reason behind further breaking the concrete is that the probability of reflective cracking decreases with the decrement of crack spacing. This method works because small concrete pieces ensure smaller gaps between them and therefore deformation is less in response to temperature changes, which lower the magnitude of critical strains at the bottom of the asphalt overlay *(28)*.

Figure 7. Rubblization size and depth: (a) Particle size viewed from the surface and (b) Influence depth seen from the side *(28)*.

3.4.3. Saw and Seal

The Saw and Seal method is ideal for increasing the longevity of asphalt pavement through the insertion of sealed control cracks that allow more expansion without causing cracks. The saw joints should cut in the asphalt no earlier than 48 hours after paving of the overlay. After sawing, the gap must be to be free from any loose particle or dust which ensures an effective seal in the joint. Sealing is recommended to construct during daylight hours and not in unfavorable weather condition *(29)*. Overlays with saw and seal treatment keep the ride quality better by slowing down the increment in IRI (International Roughness Index) than standard overlays. However, at high

cracking levels, saw and seal process is less effective in arresting the reflective cracking than overlays placed on crack-and-seat slabs. Also, saw and seal doesn't affect the amount of rutting experienced by the overlay *(30)*.

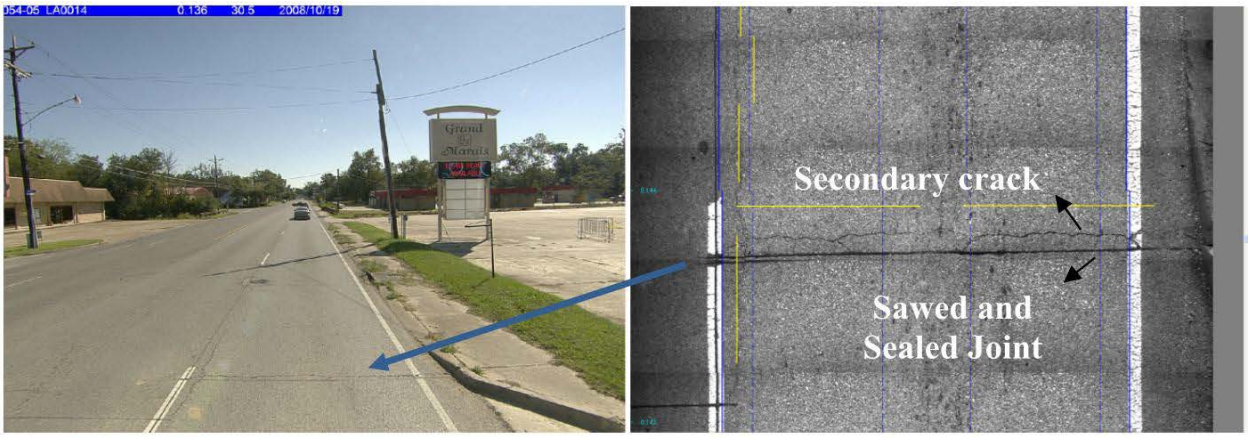

Figure 8. Illinois tollway saw-and-seal *(30)*.

3.5. Current Practice of Interlayer System

Since the early 1930s, a substantial amount of resources and efforts have been spent on finding new and economical techniques to arrest reflection crack *(9)*. Different methods, like the use of interlayer systems, have been suggested to enhance the pavement resistance to reflection cracking. In the early 1980s, the experiments showed that interlayer systems might be used to delay the reflective cracking through a new overlay placed over an old pavement *(10)*. Later, Button et al. suggested that the introduction of the interlayer to mitigate reflection cracking can be provided through two different methods:

- Reinforcing the overlay with a stiff interlayer which can provide better load distribution over a larger area and get along through the weak tensile strength of the HMA; and
- Eliminating strain energy in the cracks through the use of a soft layer *(11)*.

Generally, each treatment method is a specific target based, and all methods may not have a strengthening capability. Sometimes, treatment methods affect negatively on the performance of the pavement. The highway agencies have a strong disagreement regarding the benefits of various treatment methods due to the oversimplified view of this situation. Even sometimes, when a technique successfully delays reflection cracking, the cost is equivalent to the cost of repairing the cracks *(12)*. There are several interlayer systems which are being used in current engineering practice.

3.5.1. Geosynthetics

In the word Geosynthetics, Geo relates to the placement of the material on or in the earth or ground (e.g., in a pavement) and synthetic stands for an artificial material made by a human being. It can be anything like fabric, grid, composite, or membrane. Grids and composites are new generation materials developed for specific purposes.

Geotextiles: Fabrics or geotextiles are mainly of two types:

- Woven; and

- Nonwoven.

It is generally made of thermoplastics like polypropylene or polyester and sometimes also contain nylon and other polymers, natural organic materials, or fiberglass. Nonwoven fabrics have filaments which are typically bonded together mechanically (needle-punched) or by adhesive solutions (spun-bonded, using heat or chemicals) *(12)*. The relative performance of the geotextiles available in the market, depending on many factors related to design and construction *(31)*. The different researcher had gotten different performance matrix of geotextiles in reducing reflection cracking *(32)*, and they concluded bond between the old pavement and the new overlay had been considered an important factor *(33, 34)*. That Interfacial bond depends upon the type and amount of tack coat. Ameri et al. developed a model that shows inadequacy in interface bonding strength can cause premature overlay rutting by lateral movement of the HMA due to traffic loads *(35)*. It was also found that the micro-surfacing using modified asphalt emulsion over the fabric can not maintain a sufficient bond. They have concluded that geotextile and other types of interlayers performed considerably better in warm and mild weather than in cold climates to arrest reflective cracks (see Figure 9) *(36)* and also recommended a minimum overlay thickness of 2 inches in warmer climates. Carmichael et al. also stated from their field experience that apart from resisting the reflective cracking, the fabrics are also helpful in waterproofing the lower layer and stabilizing the subgrade moisture content *(37)*.

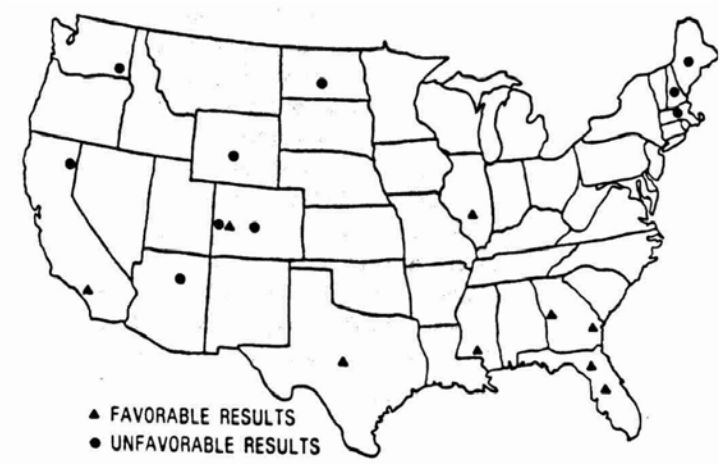

Figure 9. Locations of selected favorable and unfavorable paving fabric installations in the United States *(36)*.

Geogrids: Grids (mesh or geonets) are woven glass fibers or polymeric (polypropylene or polyester) filaments. They can be pressed or cut down from plastic sheets, and then post tension force is applied to maximize strength and modulus. Grids typically are rectangular with opening width from ¼ inch to 2 inches. Previously manufactured polymer grids were stiff and often buckled and protrude through the surface of the overlay. Some grid manufacturers have eliminated these problems by applying an adhesive to one side of his product. Even after that, proper positioning and correct installation of the grid is an essential factor for excellent performance *(37)*. Newer self-adhesive fiberglass grids are more flexible and make better positioning and proper installation is more manageable. Typically this grid has a thin membrane lamination that helps in construction (i.e., attach to the asphalt tack coat) but melts when the hot HMA overlay is applied. Nevertheless, some grids contain thin, permanent fiber strands which partially fill the apertures and adhere the grid to the tack coat without creating a waterproof barrier. Grids are designed to exhibit a high

modulus of elasticity at low strain levels such that their reinforcing benefits begin before the occurrence of tension failure of HMA overlay.

Composites and Membrane: Composites are made of a laminated fabric onto a grid. For the composite, the fabric provides absorbency to hold the asphalt and a continuous layer to ensure proper adhesion between composite and the pavement surface. The grid is also designed to provide high tensile strength and stiffness (high modulus at low strain levels). A heavy-duty membrane is also a composite system, generally made of a polypropylene or polyester mesh laminated on either or both sides of a rubber-asphalt membrane which should be impermeable. These are usually more expensive than fabrics and grid, but they offer the advantages of both of them. Membranes are typically placed in strips on joints in concrete pavements.

3.5.2. Stress Absorbing Membrane Interlayer (SAMI)

A Stress Absorbing Membrane Interlayer or SAMI is a single surface treatment consisting of a sprayed layer of asphalt and rubber binder followed by a heated stone chips application. The binder is mixed in-situ, and it contains a blend of around 80% asphalt cement and 20% crumb rubber (0.6 to 0.8 gal/yd^2 asphalt rubber material). Application of a SAMI prevents reflection of cracks through an overlay *(38)*. This overlay will behave independently from the underlying structure, which implies that, depending on its thickness, reasonable high tensile strains can be resisted the overlay and the overlay will act independently from the underlying structure. This thin overlays can be constructed instead of over thick overlays. Application of a SAMI can be made on pavements with a cracked top layer but with still enough bearing capacity of base and subgrade *(39, 40)*. The typical thickness of the SAMI ranges between 0.35 to 0.50 inch. Barksdale et al. showed that SAMI could delay reflective cracking for three to five years, but it exhibited bleeding and rutting more frequently than with the fabrics *(41)*. But according to Herbst et al. *(40)*, the overlays using SAMI can be constructed typically about 10 percent more costly than a conventional overlay.

3.6. Current Test Procedure

The reflective cracks initiate and propagate mainly because of two reasons: the passing of traffic loads and the horizontal movements due to temperature change in concrete layers *(42-48)*. Many authors suggested that the effect of thermal loading is more critical for reflective cracking than the traffic loads in an overlay *(49-56)*. There are several numbers of tests done by the various researcher to understand the procreation of cracks in the overlays, and most of them were designed to study the different systems to arrest reflective cracks, using two layer specimens with an induced crack and with the anti-reflective cracking systems placed in the interface. These tests can be differentiated by the type of applied load (i.e., traffic loads and thermal loads). Nevertheless, there are tests that evaluate both of the effects of traffic and temperature variations to determine the effectiveness of the different anti-reflective cracking systems. Generally, the tests can be divided into two segments according to the scale of the test setups:

3.6.1. Small Scale Testing

The tests which can be conducted within the scope of a laboratory, are considered as small scale tests. In this type of test, typically a model specimen of the pavement section is created in the lab. The different effects that are responsible for reflective cracking are stimulated on that specimen to

understand the various reflective cracking system. The small scale tests can be differentiated in various categories according to the test procedures:

Test Procedure Stimulating Vertical Load: Test procedures where the load is applied vertically, have the goal to stimulate the effect of traffic-induced loads. In the previous studies, the researchers used different methods which can be categorized into two distinct segments:

Passing Wheel Over the Surface: It is based on the Wheel Tracking Test. This test method evaluates the propagation of cracks in the pavement caused by the repeated passing of wheel loads. In 1993, Livneh et al. *(57)* developed the Wheel Tracking Device where a test sample of sand asphalt beam is placed upon a rubber base with a rigid bottom and gap of 10 mm at the middle. A saw cut of 30 to 40 mm deep is introduced at the bottom of the beam as a pre-crack (see Figure 10.a). After that, other researchers have utilized the same concept to test the samples with interlayers by changing the support and boundary conditions of the specimens *(58, 59)*. Gibney et al. *(58)* restrained the sample in a steel mold and used two metal plates between the specimen and the support in order to prevent the crack from initiating anywhere but in the gap between the plate (see Figure 10(b)).

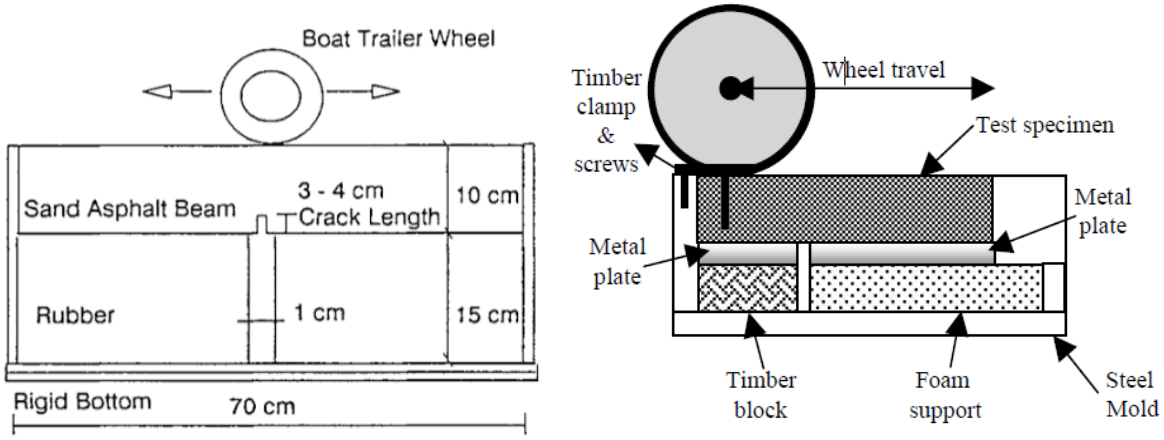

Figure 10. The laboratory Wheel Tracking Device: (a) Dimensions of the setup and (b) Test setup *(58, 59)*.

Vertical Load in Fixed Position: In other cases, the vertical loads are applied directly to the specimen at a fixed location. Within this type of tests, Denolf et al. considered the effect of the non-centered traffic loads *(60)*. They developed a new test method to simulate vertical load by a rigid prism on cement concrete slabs with an asphalt overlay. The samples used in the test, have a length of 60 cm and a width of 14 cm. They are composed of a cement concrete support with a thickness of 7 cm covered with an adhesive layer and an anti-cracking product. The reference sample, which was used to compare the effectiveness of the anti-reflective product, only an adhesive layer was used. In the end, an asphalt overlay with a thickness of 6 cm was applied as an overlay. A discontinuity of 4 mm wide was introduced in the middle of the cement concrete support to simulate the joint or a pre-crack effect.

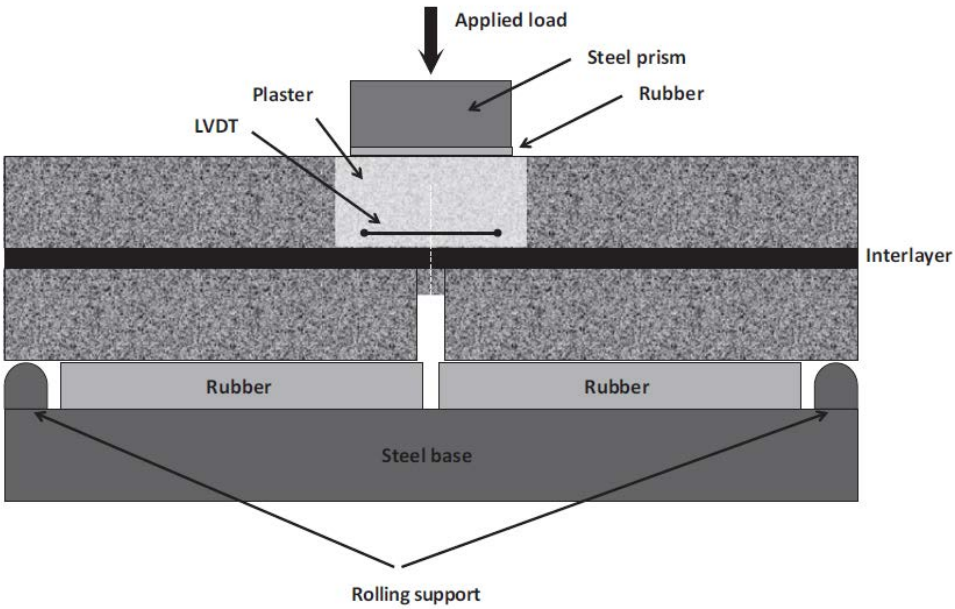

Figure 11. Diagram of the test setup and the specimen under vertical loading *(60)*.

Test Procedure Stimulating Horizontal Tension: Another important loading is introduced to the overlay is due to the effect of temperature changes. In the laboratory test setup, this kind of loading is generally stimulated through horizontal movements of the bottom of the specimen. This reciprocates the mechanisms of thermal loading by opening and closing of an induced crack. These types of tests were performed in the Belgium Laboratory of Roads (BRRC test) *(61)*, the ENTPE test *(62)* or the test of the University of Illinois *(63)*. In all these tests, the effect of Mechanically Induced Thermal Strain on the Specimen had been measured. For example, for the test setup made in the University of Illinois, The testing equipment and the arrangement of the materials are shown in Figure 12. The testing setup consists of one fixed box and a horizontally movable box on rollers. A pavement section 15.2 cm wide and 2.28 m long consisting of a 12.7-cm thick PCC slab, an Interlayer Stress Absorbing Composite (ISAC) layer, and 6.3 cm of AC was placed on top of the two box sections. A hydraulic ram attached with the movable box can open and closes the PCC slab joint to simulate seasonal or daily temperature variations. The force exerted by the hydraulic ram and the relative movement between the fixed and movable box sections can be noted by a load cell and a Linear Variable Differential Transducer (LVDT). The entire system was placed in a chamber at a temperature of −1.1°C during testing.

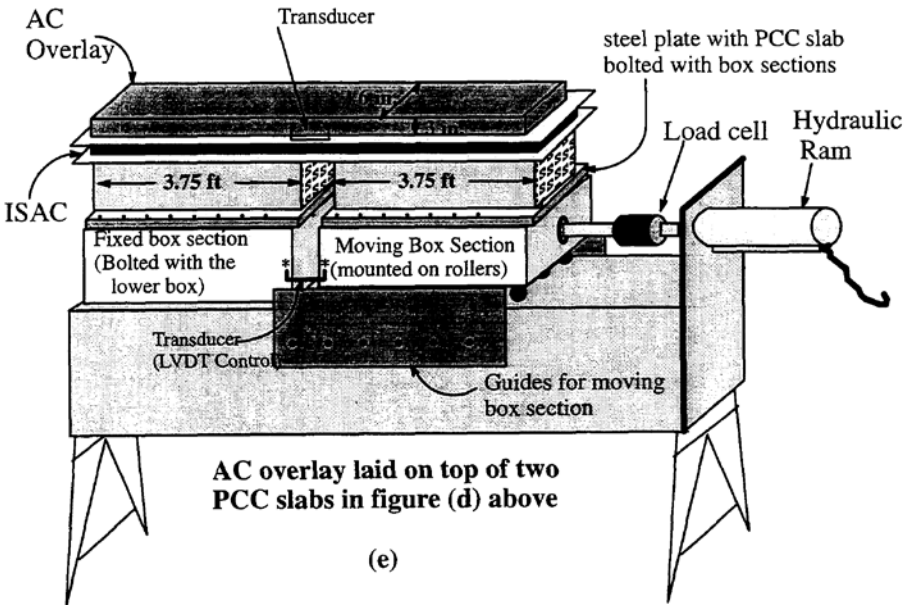

Figure 12. Testing of the overlay against thermal cracking *(63)*.

In Texas Transportation Institute (TTI) overlay testing project *(64)*, an upgraded overlay tester was developed to test smaller samples (150 mm diameter) that could be easily manufactured in the lab using a gyratory compactor or collect from standard field cores. The modified overlay test apparatus (see Figure 13) has of two steel plates, one fixed and the other can move horizontally to simulate the opening and closing of joints or pre-cracks in the old pavements beneath an overlay. In TTI, they used two setups; one is for a smaller specimen size of 15 in (375 mm) by 3 in (75 mm) with different height; the other is for larger size specimen of 20 in (500 mm) by 6 in (150 mm) with variable height.

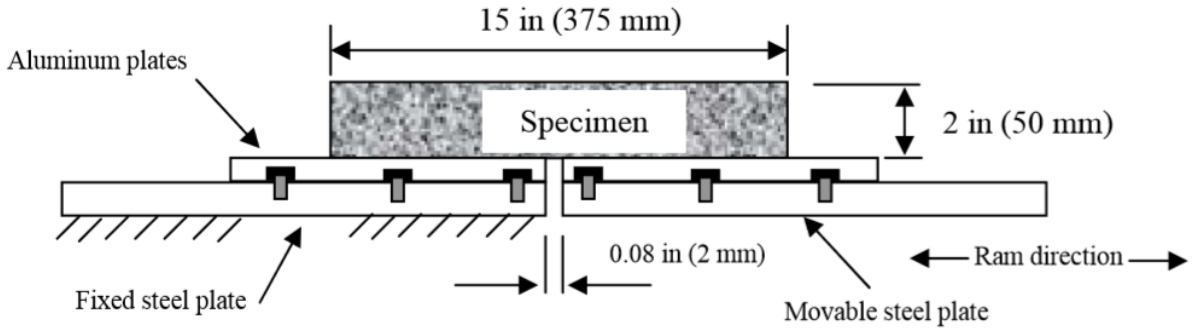

Figure 13. Conceptual figure of overlay tester *(64)*.

Test Procedure Stimulating Combination of Forces: There are some laboratory tests which perform the combination of the traffic and thermal loading, by applying vertical loads and horizontal displacements of the crack opening. Some other tests as the Reflective Cracking Device *(65)* and the test from Autun Laboratory *(66)*, a slow horizontal displacement and a vertical cyclic load at a higher frequency simultaneously applied on the Specimen. Other tests like Prieto et al. developed the Wheel Reflective Cracking (WRC) Test *(67)* were bending, tensile and shear

stresses are produced together by mobile support on which the test specimen is placed. However, the thermal effect is simulated by an opening and closing movement and the traffic load through the continuous passing of a wheel (at a rate of 43 passes/min) on the specimen surface (see Figure 14). They used 305mm x 305mm samples with a variable thickness ranging from 40mm to 80 mm for testing. They defined an empirical definition of failure based on loss of load transfer by the 0.2mm crack movement.

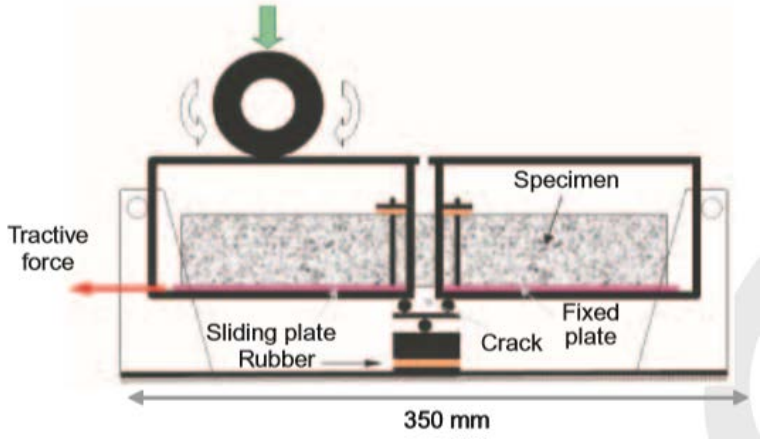

Figure 14. Diagram of the WRC Test *(67)*.

In some of the most recent studies, Moreno-Navarro and Rubio-Gámez in 2013 *(68)* have developed the UGR-FACT test where they used a new laboratory device to study the effect of tensile and shear stress due to the traffic loads and the tensile strains that are introduced by the thermal contractions. They developed a test device (see Figure 15) that proposes fatigue cracks by stimulating the stress that might affect the bitumen overlay during its design life. The device consists of a base, two sliding supports, and a load application plate. The bottom has two sloping surfaces and two rails that allow the sliding support to change position with any residual movement. With the Independent load application head and the simple geometry of the test device, it is straightforward to generate and measure vertical as well as horizontal deformation in the specimen with a dimension of 200mm x 60mm x 60mm. They have studied the behavior of different anti-reflective cracking systems using this method, but they had used a single frequency to simulate both of the effects *(69)*.

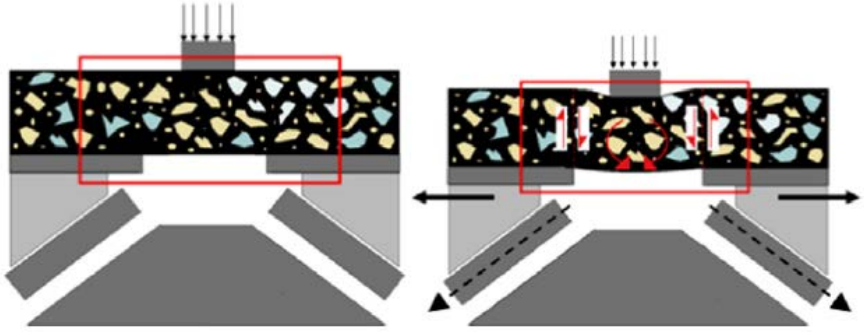

Figure 15. UGR-FACT Test Setup *(68)*.

Test Procedure Stimulating Dynamic Load: Some authors *(2, 69)* have studied either or both static and dynamic loads in a single test setup to study the effectiveness of various interlayers. They admitted that the loading should not have a constant amplitude to study the fatigue life of the specimen. Torre et al. did an experimental setup where the test device combines high and low-frequency loads, i.e., 0.005 Hz triangular load and 10 Hz senoidal load (see Figure 16) to simulate both thermal and traffic effects. In this case, only vertical loads are applied to simulate both effects. Unlike the tests carried out in other researches, here's two loads with different frequencies and amplitudes are superpositioned by a rigid prism of 100mm width on a relatively smaller scale specimen with a plan dimension of 260mm X 410mm of each layer *(71)*. The entire loading system is applied on the specimen using Universal Testing Machine (UTM) which is an advantage since the accuracy of the applied load and frequency can be assured without any particular device or set up dedicated for this test.

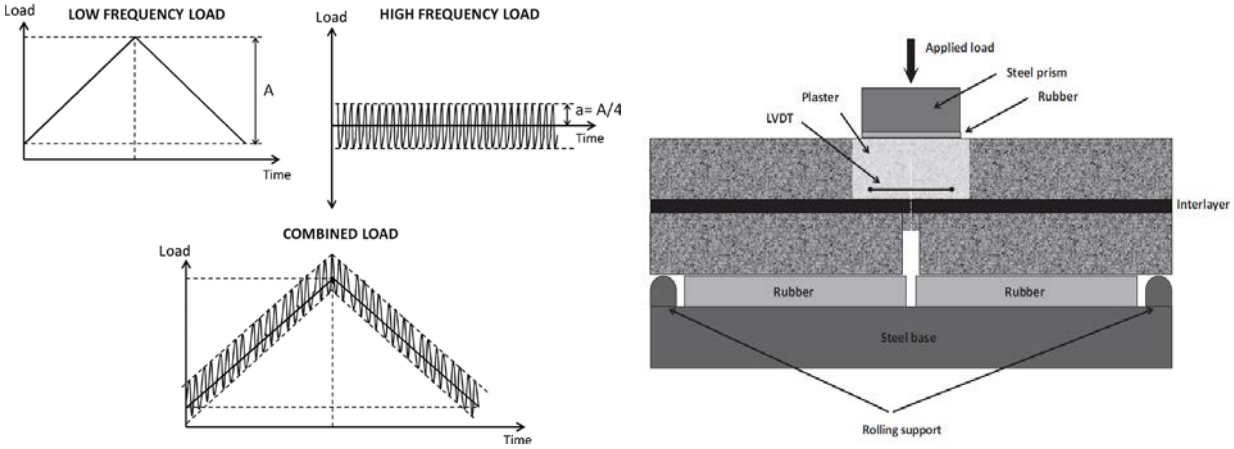

Figure 16. The diagram of: (a) Applied load frequency and (b) Test setup *(71)*.

3.6.2. Large Scale Testing

In the large scale testing, the anti-reflective cracking systems are installed in different stretches of pavement under the same physical and loading condition. Researchers collect data from those pavements and conduct a comparative study of the response of the anti-reflective cracking system. Morian et al. conducted a study in Pennsylvania to evaluate the performance of Stress Absorbing Membrane Interlayer (SAMI) and cold-in-place recycling. They installed them in a total of 49 different sections, and cost-effectiveness of these two systems was evaluated through this study *(72)*. Greene et al. did a large scale testing of the feasibility of Asphalt Rubber Membrane Interlayer (ARMI) for the Department of Transportation, Florida (FDOT). They used Accelerated Pavement Technique (APT) and long-term field performance of the experimental project to evaluate the performance of that interlayer system. In FDOT's ATP program, a Heavy Vehicle Simulator (HVS) had been used. It was capable of applying 7 to 45 kip load along a 20-feet long test strip (see Figure 17) *(73)*.

Figure 17. HVS and APT test tracks for FDOT *(73)*.

3.7. ECC Interlayer System

Engineered Cementitious Composite or ECC is a type of High-Performance Fiber-Reinforced Cementitious Composite (HPFRCC) with high ductility. It was initially developed for the applications in the cost-sensitive and construction with massive material volume usage, but for a decade ECC has undergone through significant evolution through a significant evolution in both the range of application and material development. ECC gives an extraordinarily high performance as an advance construction material. Comparing the behavior of conventional concrete, fiber reinforced concrete (FRC) and ECC under tension (see Figure 18) *(74)*, the traditional concrete shows a brittle failure and the FRC exhibits a softening behavior post the first crack while a pseudo-strain hardening behavior in ECC is experienced under the same test conditions *(75)*.

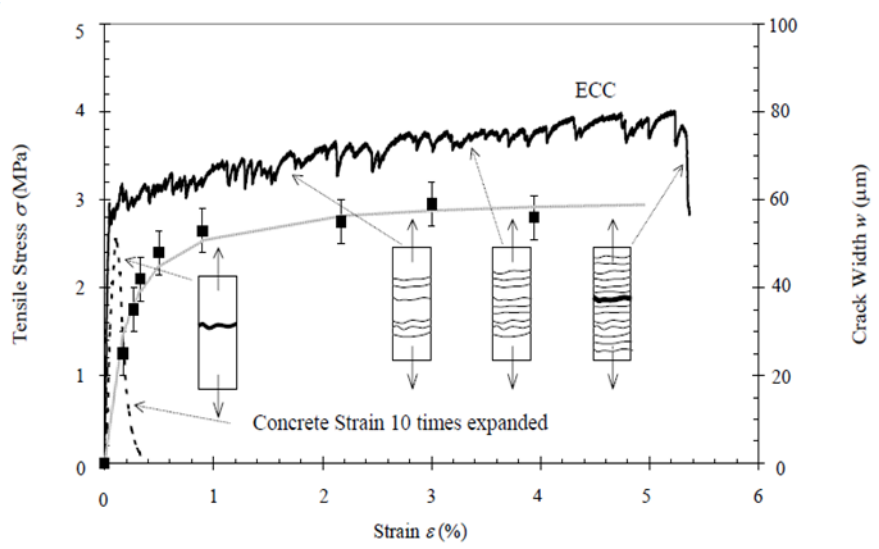

Figure 18. Typical ECC tensile stress-strain curve and multiple cracking behaviors *(74)*.

It provides a remarkable contribution to structural ductility, deformation capacity, strength, damage tolerance, and repairability *(76)*. It also has a high shear capacity *(77)* and superior durability performance under various environmental loadings including chloride attack, sulfate attack, hot and humid environment, accelerated corrosion, and freezing and thawing cycles *(78)*. ECC even can deliver compatible deformation with multiple small cracks width limited to below 0.2mm. *(79)* while concrete and FRC failed with single localized cracking.

Typical ECC material consists of cement, silica sand, fly ash, water, admixtures, and polymeric fibers (polyvinyl alcohol (PVA) fibers, polyethylene (PE) fibers, etc.). Polyvinyl Alcohol (PVA) fiber is a type of fiber which is made from Polyvinyl alcohol through wet spinning, heat treatment, and crimping-oil in the water at normal temperature. It shows good physical, mechanical property, and dry heat stability. Another essential characteristic of the PVA fiber is solubility in water at a range of temperature. Typically, it has a tensile strength between 1600 and 2500 MPa, but the cost is almost 1/8th of the conventional Poly Ethylene (PE) fiber. Due to its hydrophilic nature, PVA fiber shows strong affinity to hydroxy groups in hydrated cement and it results in strong chemical bond which allows tailoring of material to achieve energy and strength balances between fiber, matrix, and interface properties to have a higher tensile strain capacity at moderate fiber content (less than 2%) *(80)*.

While comparing to the concrete overlay system and the HMA overlay system, ECC overlay system reduces greenhouse gas emissions by 32% and 37%, total life cycle energy by 15% and 72%, total life cycle energy by 15% and 72%, and costs by 40% and 58%, respectively, over the entire 40-year life cycle *(81)*. But when we consider the initial cost of construction, constructing an entire overlay with ECC is not an economical solution due to its high material cost. The relatively high material cost of ECC is mostly associated with the high cost and lack of local availability of raw ingredients including polymer fibers and fine silica sand. and that's why ECC can be installed an interlayer system instead of an overlay with locally available cost-effective materials.

In recent years, cost-effective ECC mixtures with sufficient tensile ductility were developed by a various researcher with locally available PVA fibers (typically with no surface oil coatings) *(82)* and local sands with coarser particle size than silica sand *(83)*. Nevertheless, it has found that due to typically 2-3 times higher cement usage in the ECC than normal cement causes higher autogenous shrinkage, the heat of hydration and material cost. To overcome these impacts, in ECC design, a significant portion of cement can be replaced with industrial by-product like fly ash, slag and surprisingly, it does not compromise the mechanical properties of ECC; somewhat, it often improves the performance *(84)*. Yang et al. *(85)* tested the mechanical performance of ultra-high volume fly ash with cement replacement up to 85% by weight. Even at such high fly ash content, ECC retained the tensile ductility of approximately 2 to 3% and exhibits strain capacity in the range of 3-5% *(86)* compared to 0.01% for ordinary concrete (see Figure 19). Additionally, the results showed that with the increment of fly ash content, crack width, and free drying shrinkage reduced. Matrix densification occurred due to pozzolanic property, shape, and micro-filler effect of fly ash. Also, the un-hydrated fly ash particles served as fine aggregate to restrain the shrinkage behavior *(87, 88)*.

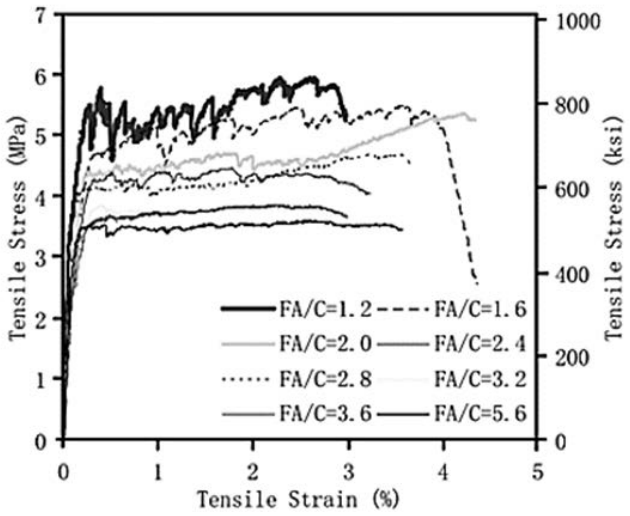

Figure 19. Representative tensile stress-strain cure of HVFA ECC tested at 28 days *(85)*.

The compressive strength of ECC varies in between the range of 20-165 MPa depending on the design mix of the ECC, which is similar to regular concrete. The elastic modulus of ECC is around 18-34 MPa, which is slightly lower than that of concrete as the coarse aggregates are not used in the ECC mix. The highly ductile tensile behavior of ECC also leads to a ductile flexural response *(84)*. Due to multiple crack formation on the tension side under bending allows ECC to attain large curvature and deflection capacity (see Figure 20) without failure and thus it is often referred to as bendable concrete *(89)*. That's why it is hypothesized that ECC will provide the structural stability of the rigid interlayers and reduce the strain energy at the bottom of the overlay just like soft interlayers.

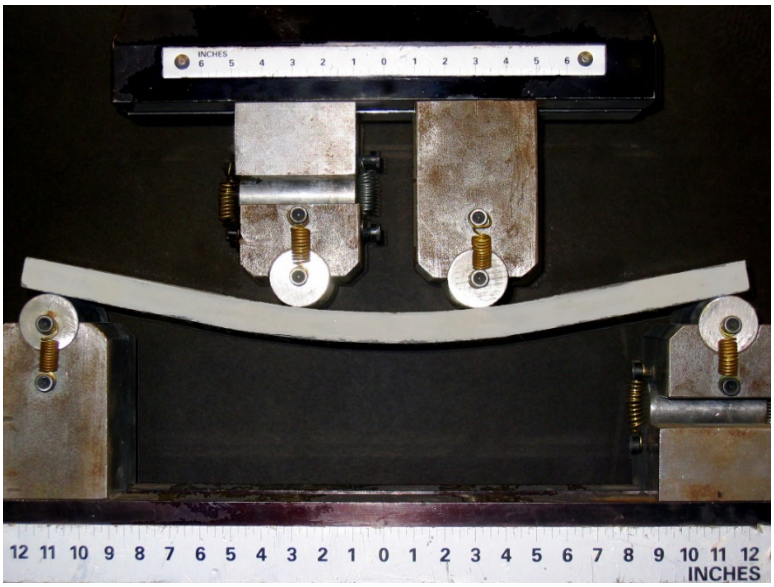

Figure 20. Flexural response of ECC *(89).*

A summary of significant mechanical properties of ECC is shown in Table 1. ECC mix is tailorable according to specific application requirement, maintaining the feature of high tensile ductility is maintained, through the guidance of the micromechanics design principle.

Table 1. Mechanical properties of ECC *(90, 91).*

Compressive Strength (MPa)	First Cracking Strength (MPa)	Ultimate Tensile Strength (MPa)	Ultimate Tensile Strain (%)	Flexural Strength (MPa)	Young's Modulus (GPa)
20-165	3-8	4-15	1-8	10-30	18-34

With all above-mentioned characteristics, It has been seen that Engineer Cementitious Composite (ECC) has excellent potential as an interlayer system causes significant improvement at any stress level compared to other types of interlayers.

4. METHODOLOGY

4.1. Materials and Specimen Preparation

4.1.1. Hot-Mix Asphalt (HMA)

Superpave mixture design was conducted for HMA mixture. The mix design yielded 4.75% optimum asphalt content for the target air void of 4%. PG64-22 and limestone aggregates were acquired from a local contractor. The aggregate gradation used for HMA mixture is shown in Table 2.

Table 2. Aggregate gradation used for the HMA mix.

Sieve (mm)	Passing (%)
12.5	100
9.5	94
No. 4	85
No. 8	68
No. 16	46
No. 30	25
No. 50	14
No. 100	8
No. 200	3

4.1.2. HMA Beam Specimen

HMA beam specimens of 51mm x 51mm x 305mm were prepared using 90 kN (20 kips) dynamic press machine. The loose HMA mixture heated at compaction temperature of 150-degree Celsius was poured into a steel mold. The top plate of the dynamic press machine was allowed to sit on the steel compaction beam and then a ramp load of 20 kN was slowly applied. After initial compaction, a cyclic load using Haversine waveform was applied, where maximum and minimum loads were 65 kN and 2 kN, respectively. The cyclic load over the specimen was released after the required thickness to achieve target density was obtained. The above procedure yielded uniform beam specimens of about 51 ± 2 mm thickness and air void content of 4 ± 0.25%.

4.1.3. Engineered Cementitious Composite (ECC)

The material used to develop ECC mixture is Type 1 Portland cement, class F fly ash, river sand, water, high range water reducing admixture, and Polyvinyl Alcohol (PVA) fibers. The mix proportion is summarized in *(19)*.

Table 3. Mix design of ECC (kg/m^3).

Mix ID	Cement (gm)	Fly Ash (gm)	River Sand (gm)	Water (gm)	Admixture (gm)	PVA Fiber (2% by Volume) (gm)
FA 3.2	302	965	467	329	3.6	26

To construct ECC, all the solid ingredients were thoroughly dry-mixed for 2 min. Water was then gradually added and mixed for another 2 min followed by a water reducer agent as per need to achieve a workable paste. After reaching the required consistency, fibers were added slowly and blended carefully for another 4 to 6 min. The mixture was then poured on plate molds of 305mm x 51mm x 12.5mm to prepare 12.5 mm and 6.25 mm thick ECC specimens. The ECC used in this study was designed based on locally available material with an average tensile strength of 2.4 MPa and tensile strain capacity of 2.5%. All specimens were cured for 28 days under standard laboratory conditions (23±3°C and 50±10% relative humidity) sealed in a plastic sheet.

4.1.4. Portland Cement Concrete (PCC)

A quick mix of concrete was used to prepare 51mm x 51mm x 152mm PCC beam as a base layer for the interlayer specimens. Two such beams 6mm apart were placed underneath the control HMA or ECC interlayer, representing a PCC joint under HMA layer.

4.1.5. Control HMA and ECC Interlayer Composite Specimen

To prepare the control specimen, the HMA and two PCC beams were preheated at 145°C for 30 min. The HMA beam was then bonded to the two PCC beams (6 mm joint at the center) using a thin layer of preheated PG64-22 asphalt binder as a tack coat. A 15 kg sustained load was placed on the top of the HMA layer for 45 min to achieve adequate adhesion. To prepare the interlayer specimen, the preheated HMA beam was bonded with the ECC interlayer beam using preheated asphalt binder as before. The ECC beam was not heated unlike the PCC beam of control specimen. The HMA and ECC combined beam were then bonded with two PCC beams using epoxy glue. It should be noted that center span of about 150mm for ECC beam was not bonded with PCC to utilize maximum strain capacity of ECC interlayer. The combined thickness of ECC and HMA was always maintained at 50 mm. HMA beams thickness was reduced by a saw-cut before it was bonded to ECC. Figure 21 shows a schematic image of an ECC Interlayer specimen.

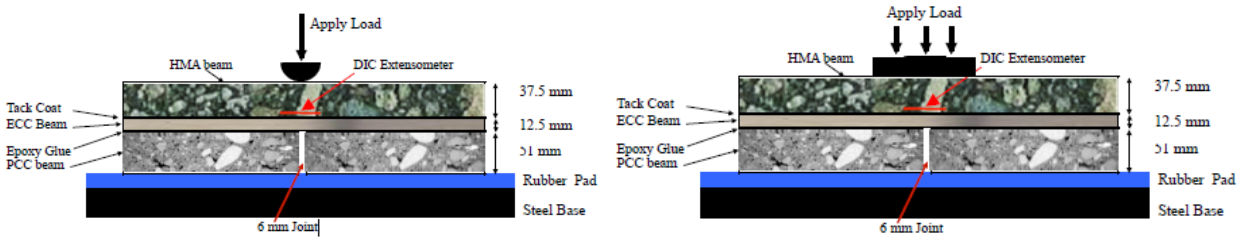

Figure 21. Specimen diagram: (a) Point load and (b) Distributed load.

4.2. Test Methods

4.2.1. Digital Image Correlation (DIC)

DIC technique is one of the ways to measure any strain in any direction on a 2D plane for a test specimen. Researchers have been using this technique to measure strain development and propagation on laboratory test specimens recently. In this technique, the specimen face is painted with densely spread black dots on a white background. From the respective displacement of black dots (in any direction) on a white surface, the strain could be measured from the following images at the time loading and unloading. Hence, horizontal/vertical or shear strains could be measured by following images of the surface and could be corresponded to loading. Using this technique, a virtual extensometer could be put on any direction and strain could also be measured at that direction *(92-95)*. Several researchers have used this DIC technique to study the strain development and propagation in different types of interlayers on pavements. With the help of the DIC technique, they also estimated fatigue lives of test specimens for the performance measure of interlayer *(97-100)*.

In this research, the DIC technique has been implemented to study the strain development and crack propagation of the HMA layer with or without ECC interlayer. With the help of the DIC technique, fatigue lives of the specimens were also measured, and the performance of ECC was evaluated.

4.2.2. Flexural Ramp Loading Test

At first, a flexural ramp loading test was performed on both ECC and control specimens to understand and compare the reflective crack development and propagation pattern. Specimens were supported uniformly by 12.5 mm thick rubber pad. The rubber pad was resting on a 50 mm thick steel base. A point load was applied at the center of the specimen at a rate of 0.5 mm/min (Figure 21). With the help of DIC camera, images were taken at every 0.25 s interval. These images were used to analyze horizontal strain distribution for the test. Triplicate specimens were tested for control, 6.25 mm, and 12.5 mm thick ECC interlayer under HMA beam.

4.2.3. Flexural Fatigue Test

Haversine load waveform with 0.1 sec of the load-unload period and 0.5 sec of rest period was used for fatigue test. Maximum and minimum applied cyclic loads were 1.0 kN and 0.1 kN, respectively. The repeated load was applied until the complete failure of the specimen. While the test was being conducted, continuous DIC images were obtained using the camera with an interval of 60 sec. With the help of DIC images, horizontal tensile strain map was drawn, and cumulative tensile strains were calculated to determine fatigue life for each specimen. For fatigue test under

distributed loading, the same load was applied to an area of 6 sq. in. (3 in. x 2 in.) in the middle of the specimen.

5. ANALYSIS AND FINDINGS

5.1. Horizontal Tensile Strain Map From Ramp Loading Test

For the flexural ramp-loading test, the horizontal tensile strain (Exx_t) map obtained from DIC is shown in Figure 22. Three different time points from the beginning of the test were chosen (T1=90 sec, T2=240 sec, T3=420 sec) for Exx_t map as shown in the figures. It is worth mentioning that this strain is a total strain, which comprises elastic, plastic and viscous strain. Flexural Stress (σ) at the bottom of the HMA layer corresponding to time is calculated and mentioned in the figure. It is clear that without any ECC interlayer, one single reflective crack propagates from bottom to top, whereas with the presence of ECC interlayer, multiple cracks propagate from the bottom of HMA and they join together at the time of failure. Furthermore, DIC images did not detect any crack in ECC interlayer at failure. It was found that the ECC interlayer specimens showed higher flexural stress level at failure (14 MPa) as opposed to the control specimens which failed at a stress level of 8.6 MPa.

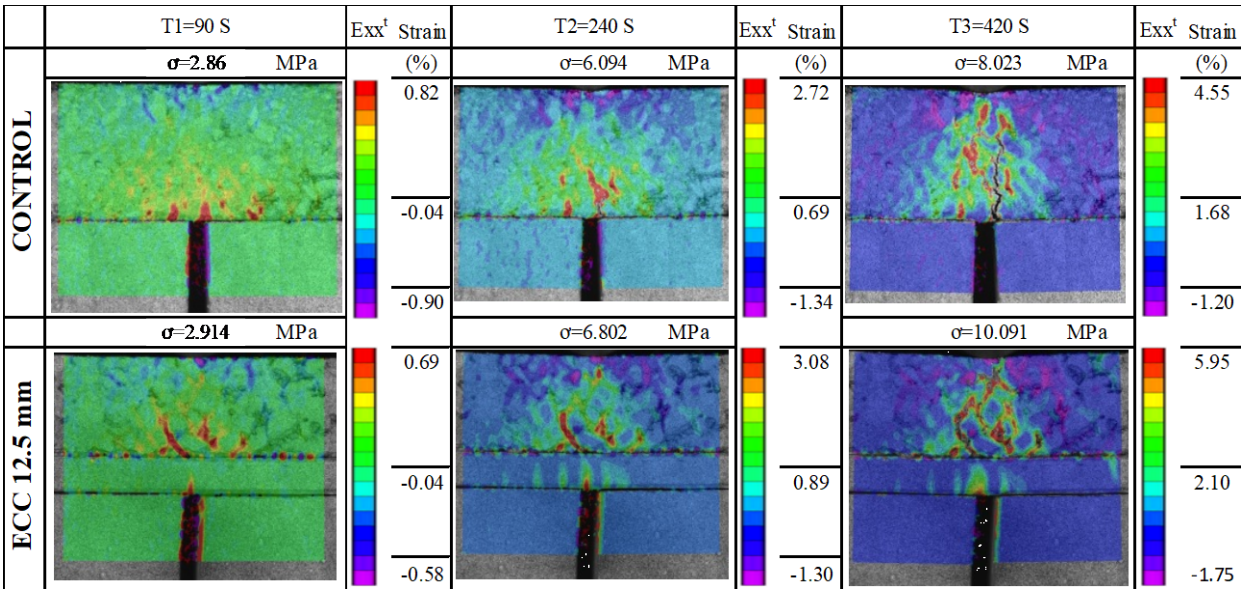

Figure 22. Distribution of horizontal tensile strain (Exxt) for control and ECC Interlayer specimens.

5.2. Fatigue Life

From the fatigue test specimens, the cumulative horizontal tensile strain (Exx_c) is calculated from DIC images for each cycle at the bottom of the HMA layer. Location of virtual extensometer for Exxc calculation is shown in Figure 21 by a red line at the center-bottom of the HMA layer. Figure 23 illustrates a comparison of cumulative horizontal tensile strains (Exx_c) as a function of load cycles for both ECC interlayer and control specimens.

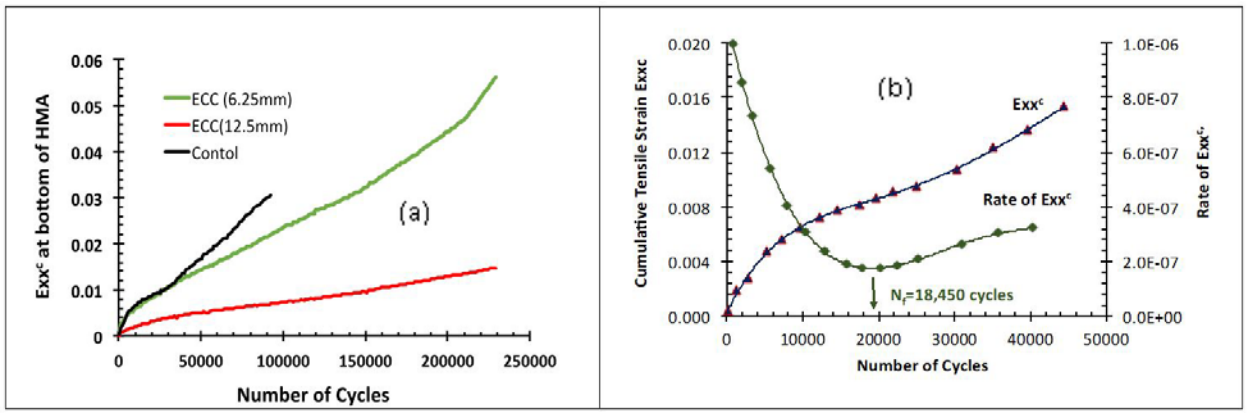

Figure 23. Analysis results: (a) Cumulative tensile strain comparison and (b) Fatigue life determination.

It can be seen in Figure 23(a) that for the same load cycle, the thicker ECC interlayer of 12.5 mm exhibited significantly lower Exxc values as compared to the control ones. Similarly, for the thinner ECC interlayer of 6.25 mm, the Exxc values were lower than the control specimens during higher load cycles. Since the accumulation of tensile strain at the bottom of the HMA layer was much lower for ECC interlayer system, it is expected that the fatigue life (Nf) for such mixtures will be much higher. To determine fatigue life, Exxc was plotted against the number of load cycles for each specimen as shown in Figure 23(b). The rate of strain accumulation was calculated and then plotted as a function of load cycles. It can be seen that the rate of accumulation decreased first, reached a minimum value and then started to increase. It is assumed that the increase in the rate is due to microcrack initiation and propagation. The number of load cycles at which the rate of cumulative tensile strain just started to increase was reported as the fatigue life of the specimen as shown in Figure 23(b). The fatigue lives of the control and ECC interlayer specimens were determined and compared as shown in Table 4. It is obvious that the ECC interlayer specimens exhibited approximately 70% and 140% average increase of fatigue lives, for 6.25 mm and 12.5 mm thick ECC, respectively. This indicates that the ECC interlayers were successful in distributing the stresses to a wider area. Thus, resulting in lower tensile strains at the bottom of the HMA layer and delaying the microcrack initiation, formation of macrocracks and propagation as reflective cracks.

Table 4. Summary of fatigue life of control and ECC interlayer systems under point load.

Specimen Type	Average	Standard Deviation	Co efficient of Variation (%)
Control	27,400	8,950	32.66
ECC interlayer 6.25 mm	46,500	750	1.62
ECC interlayer 12 mm	65,000	1,850	2.85

For the fatigue test specimens, the cumulative horizontal strain map comparison for control, ECC 6.5 mm and ECC 12.5 mm interlayer at 36,000 and 84,000 cycles are shown in Figure 24. By 36,000 cycles, the control specimen failed as the rate of strain (Exx_c) accumulation started to increase rapidly and crack initiation was also detected by DIC. On the contrary, the ECC 6.25 mm specimen did not reach fatigue life as its rate of strain (Exx_c) did not start increasing by this time. The strain map is also showing that the ECC 6.5 mm has distributed the strains (Exx_c) on a wider

area with respect to the control specimen. Maximum strain level for ECC 6.25 mm specimen was slightly less than the control specimen at this stage. ECC 12.5 mm showed a significantly lower maximum strain (1.48%) at this stage and were not even nearer to fatigue life. ECC 12.5 mm also distributes the strains to a wider area like the 6.25 mm specimen.

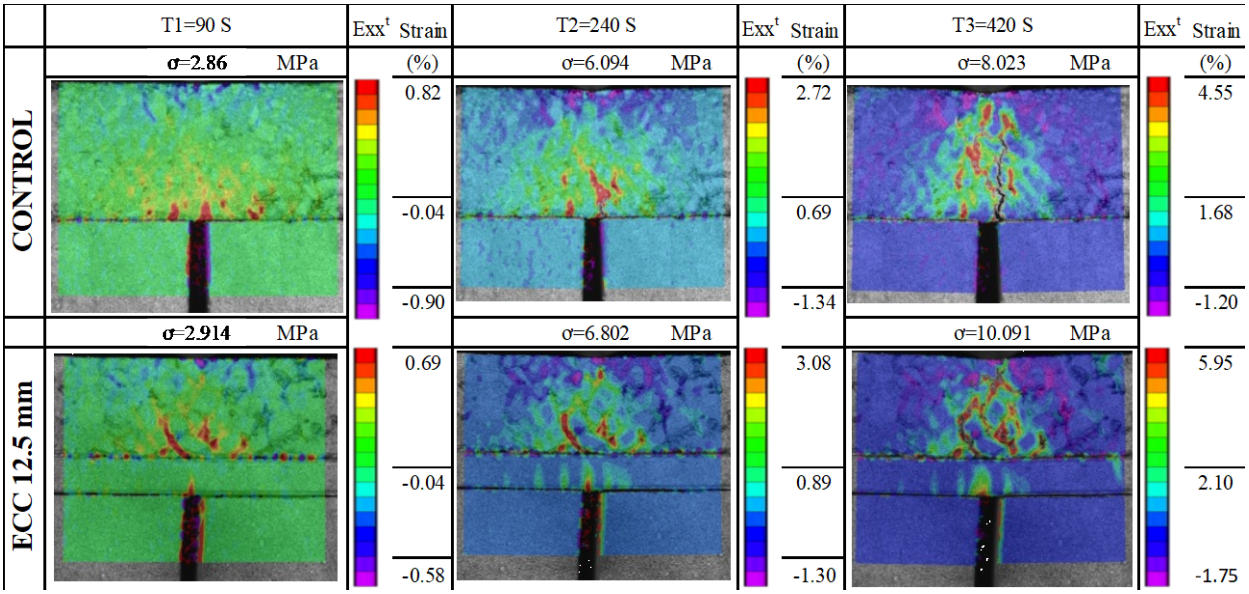

Figure 24. Distribution of horizontal tensile strain under fatigue loading.

One single reflective crack is clearly visible at 84,000 cycles for the control specimen, but ECC 6.25 mm specimen did not show a full depth crack at this time although the specimen exceeded its fatigue life. This implies that the ECC 6.25 mm specimen takes a longer time to generate a full crack after the crack initiation. In other words, ECC delays crack propagation and full crack development. Although ECC 12.5 mm exceeded its fatigue life at 84,000 cycles due to an increased rate of strain, it shows thin crack initiation lines at this stage. It is also noticeable that ECC itself did not show any crack or plastic strain in these images.

Three ECC interlayer and three control samples were also tested under distributed loading. The control samples failed in reflective cracking just like the samples under point load but the ECC specimens did not fail in reflective crack failure. The crack initiated at the top of the specimen and propagated towards the bottom and showed similar strain comparison pattern (see significant improvement in fatigue life).

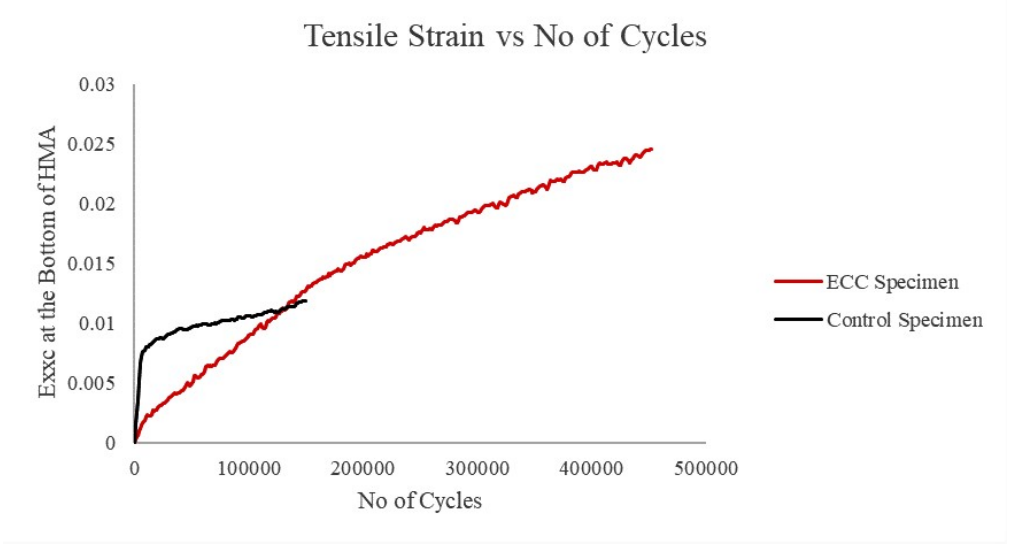

Figure 25. Cumulative tensile strain comparison of specimens under distributed loading.

5.3 Cost Analysis

For lifecycle cost analysis, the following assumptions were made:

- The fatigue life improved by 300% for laboratory HMA specimen using the high-performance fiber reinforced cement composite (HPFRC) interlayer system for concentrated load condition. Even though it is difficult to quantify the actual field performance from laboratory data, it is expected that such improvements may lead to the pavement service life extension of about 100%.
- Composite pavement with HMA application of 3.5”over PCC base for Arterial system is used in this comparison.

The following calculations were made:

- Cost of 3.5” HMA over PCC base/lane-mile = $225,000;
- Service life of such composite pavement = 8 yr;
- Cost of HPFRC interlayer 2’ wide placed on each Joint (16’ spacing)/ lane-mile = $5,000;
- Service life of pavement with HPFRC interlayer (100% increase) on PCC joints = (2*8) = 16 yr;
- Cost /lane-mile/year of 3.5” HMA on PCC = ($225,000/8) = $28,125;
- Cost /lane-mile/year of 3.5” HMA with HPFRC interlayer on PCC joints = ($230,000/16) = $14,375;
- Cost Reduction/lane-mile/year = ($28,125 - $14,375) = $13,750; and
- % Reduction in Cost /lane-mile/year = ($13,750/$28,125)*100 = 49%.

6. CONCLUSIONS

To mitigate the reflective cracking in the HMA overlay constructed on top of deteriorated concrete pavement, the introduction of a thin layer of Engineered Cementitious Composite was found effective. For the laboratory experimentation, The improvement in the test specimens with ECC interlayer was evaluated under fatigue loading condition, and the result was compared with the test specimens without ECC interlayers without changing loading conditions. To understand the behavior of the ECC as an interlayer, two different bonding conditions were established, i.e., fully bonded and half bonded between the ECC and the PCC underlay. A Direct Image Correlation method was employed to study the strain maps, crack initiation and propogation.

Based on the results and discussion, the following conclusions were made:

- ECC interlayer significantly delays reflective crack growth by providing a firm base underneath the HMA. It was found that thicker ECC interlayer (12.5 mm) increased fatigue life by 140% while the thinner ECC interlayer (6.5 mm) showed 70% improvement under point load.
- Horizontal tensile strain map as observed from DIC images for both ramp loading and fatigue test has illustrated that the ECC interlayer distributes the stress concentration at the joint to a broader area. For fatigue test, ECC reduced the tensile stress level on the bottom of HMA, which delayed reflective crack initiation, propagation, and acceleration. This delay ultimately increased the fatigue life of the ECC specimen.
- It was found that instead of one single reflective crack as observed in the control specimen, ECC interlayer specimen under point load generated multiple reflective cracks, which were merged at failure. But in case of distributed load, ECC interlayer specimen cracks were generated at the top of the HMA and propagated downward.
- ECC interlayer beam did not show any significant strain and crack during ramp loading and fatigue tests. It was observed that the crack initiated and propagated through the HMA only.

The results of the experimentation indicate that ECC has high potential to be used as an interlayer system to mitigate reflective cracking in composite Pavements. However, the current study only focuses on small scale lab testing under repeated loadings, in order to adopt this technology in the field, additional evaluation such as shear or interface failure between ECC and HMA layer, and full scale pavement testing and validations are needed.

REFERENCES

1. Dhakal, N., Elseifi, M.A. and Z. Zhang (2016). Mitigation strategies for reflection cracking in rehabilitated pavements–A synthesis. *International Journal of Pavement Research and Technology,* 9(3), pp. 228-239.

2. Hughes, J.J. and I. Al-Qadi (2001). *Evaluation of Steel Paving Mesh*. No. FHWA-PA-2002-001+ 2000-058, FHWA, U.S. Departmention of Transportaiton.

3. Button, J. and R. Lytton (2003). *Field Synthesis of Geotextiles in Flexible and Rigid Pavement Overlay Strategies Including Cost Considerations*. Texas Transportation Institute, College Station, Texas.

4. Lytton, R.L. (1989). Use of geotextiles for reinforcement and strain relief in asphalt concrete. *Geotextiles and Geomembranes*, Vol. 8, pp. 217-237

5. Elseifi, M.A. and I.L. Al-Qadi (2003). A simplified overlay design model against reflective cracking utilizing service life prediction. *Roads Materials and Pavement Design*, Vol. 5(2), pp. 169-191.

6. Sheng, H., Zhou, F., and T. Scullion (2010). Reflection cracking-based asphalt overlay thickness design and analysis tool. *Transportation Research Record: Journal of the Transportation Research Board*, Vol. 2155(1), pp. 12–23.

7. Cleveland, S.G.. Lytton, R.L., and J.W. Button (2002). Reinforcing benefits of geosynthetic materials in asphalt concrete overlays using pseudo strain damage theory. In *82nd Annual Meeting of the Transportation Research Board*, Transportation Research Board, Washington, D.C.

8. Mukhtar, M.T. and Dempsey, B.J., 1996. Interlayer stress absorbing composite (ISAC) for mitigating reflection cracking in asphalt concrete overlays (No. UILU-ENG-96-2006).

9. Pierce, L.M., Jackson, N.C., and J.P. Mahoney (1993). Development and implementation of a mechanistic, empirically based overlay design procedure for flexible pavements. *Transportation Research Record: Journal of the Transportation Research Board*, Vol. 1388.

10. Chan, F., Barksdale, R.D. and S.F. Brown (1989). Aggregate base reinforcement of surfaced pavements. *Geotextiles and Geomembranes*, 8(3), pp.165-189.

11. Khodaii, A., Fallah, S., and F.M. Nejad (2009). Effects of geogrid on reduction of reflection cracking in asphalt overlays. *Geotextiles and Geomembranes*, 27(1), pp. 1-8.

12. Huges, C.S. and K.H. McGhee (1973). *Results of Reflection Crack Questionnaire Survey*. Report No. VHRC, pp.72-R25.

13. Bayomy, F.M., Al-Kandari, F.A. and Smith, R.M., 1996. Mechanistically based flexible overlay design system for Idaho. Transportation Research Record, 1543(1), pp.10-19.

14. Lee, E.B., Ibbs, C.W., Harvey, J.T., and J.R. Roesler (2000). Construction productivity and constraints for concrete pavement rehabilitation in urban corridors. *Transportation Research Record: Journal of the Transportation Research Board*, Vol. 1712(1), pp. 13-22.

15. Wang, T., Lee, I.S., Kendall, A., Harvey, J., Lee, E.B. and C. Kim (2012). Life cycle energy consumption and GHG emission from pavement rehabilitation with different rolling resistance. *Journal of Cleaner Production*, 33, pp.86-96.

16. Finn, F.N., and C.L. Monismith (1984). Asphalt overlay design procedures. *NCHRP Synthesis 116*, National Cooperative Highway Research Program, National Research Council, Washington, D.C.

17. Gulden, W., and D. Brown (1984). Overlays for plain jointed concrete pavements. No. 7502, Georgia Department of Transportation.

18. Predoehl, N.H. (1989). Use of paving fabric test installations in california. California Department of Transportation, Translab.

19. McLaughlin, A.L. (1979). Reflection cracking of bituminous overlays for airport pavements; A state of the art. No. FAA-RD-79-57), FAA, U.S. Department of Transportation.

20. Button, J.W. and T.G. Hunter (1984). Synthetic fibers in asphalt paving mixtures. Report No. 319-1F, Texas Transportation Institute, College Station, TX.

21. Beckham, W.K. and W.H. Mills (1935). Cotton-fabric-reinforced roads. *Engineering News Record*, Vol. 115(13), pp. 453-455.

22. Leng, Z., Al-Qadi, I.L., Carpenter, S.H., and H. Ozer (2009). Interface bonding between hot-mix asphalt and various portland cement concrete surfaces. *Transportation Research Record: Journal of the Transportation Research Board*, No. 2127, pp. 20-28.

23. Wen, H., Titi, H., and J. Singh (2005). Guidelines for the surface preparation/rehabilitation of existing concrete and asphaltic pavements prior to an asphaltic concrete overlay. Report No. 0092-04-05, Wisconsin Highway Research Program, Madison WI.

24. Thompson, M.R. (1999). Hot-mix asphalt overlay design concepts for rubblized portland cement concrete pavements. *Transportation Research Record: Journal of the Transportation Research Board*, Vol. 1684(1), pp. 147-155.

25. Freeman, T.E. (2002). Evaluation of concrete slab fracturing techniques in mitigating reflective cracking through asphalt overlays. No. VTRC-03-R3, Virginia Transportation Research Council, Charlottesville, VA.

26. Galal, K.A., Coree, B.J., Haddock, J.E., and T.D. White (1999). Structural adequacy of rubblized portland cement concrete pavement. *Transportation Research Record: Journal of the Transportation Research Board*, No. 1684, pp. 172-177.

27. Ceylan, H., Mathews, R., Kota, T., Goplalkrishnan, K. and B. Coree (2005). Rehabilitation of concrete pavements utilizing rubblization and crack-and-seat methods. Iowa Highway Research Board Report No. TR-473, Center for Transportation Research and Education, Ames, IA.

28. Khedaywi, T.S. and T.D. White (1996). Effect of segregation on fatigue performance of asphalt paving mixtures. *Transportation Research Record: Journal of the Transportation Research Board*, Vol. 1543, pp. 63–70.

29. Rao, S., Darter, M.I, Tompkins, D., Vancura, M., Khazanovich, L., Signore, J., Coleri, E., Wu, R., Harvey, J., and J. Vandenbossche (2011). Composite pavement systems, Final report with appendices. *Strategic Highway Research Program 2*, Transportation Research Board of the National Academies, National Research Council. Washington D.C.

30. Hall, K., Correa, C. and A. Simpson (2005). LTPP data analysis: Effectiveness of maintenance and rehabilitation options. *NCHRP Web Document 47*, National Cooperative Highway Research Program, Transportation Research Board, Washington, D.C.

31. Holtz, R.D., Christopher, B.R., and R.R. Berg (1998). Geosynthetic design and construction guidelines. Publication No. FHWA HI-95-038, NHI Course No. 13213, NHI, FHWA, U.S. Department of Transportation.

32. Barksdale, R.D. (1991). Fabrics in asphalt overlays and pavement maintenance. *NCHRP Synthesis 171*, National Cooperative Highway Research Program, National Research Council, Washington, D.C.

33. Ni, M. and Z. Yao (1989). Stress analysis of asphalt overlays on existing concrete pavements. *Journal of Tongji University*, Tongji University, Shanghai, China.

34. Brown, S.F., N.H. Thom, and P.J. Sanders (2001). A study of grid reinforced asphalt to combat reflection cracking. In *Proceedings of Association of Asphalt Paving Technologists*, Vol. 70.

35. Ameri-Gaznon, M. and D.N. Little (1988). Permanent deformation potential in asphalt concrete overlays over portland cement concrete pavements. No. 452-3F, Texas Transportation Institute, College Station, TX.

36. Ahlrich, R.C. (1986). Evaluation of asphalt rubber and engineering fabrics as pavement interlayers. No. WES/MP/GL-86-34. Army Engineer Waterays Experiment Station, Vicksburg, MS.

37. Kennepohl, G.J.A. and N. Kamel (1984). Construction of tensar reinforced asphalt pavements. In *Proceedings of Science and Engineering Research Council*, London, England.

38. Molenaar, A.A.A., Heerkens, J.C.P., and J.H.M. Verhoeven (1986). Effects of stress absorbing membrane interlayers. In *Association of Asphalt Paving Technologists Proceedings*, Vol. 55.

39. Kuang-huai, W.U. (2006). Study on design and performance of stress absorbing membrane interlayer (SAMI) mixture. *Journal of Highway and Transportation Research and Development*, Vol. 23(12), pp.18-20.

40. Herbst, G., H. Kirchknopf, and J. Litzka (1993). Asphalt overlay on crack-sealed concrete pavements using stress distributing media. In *RILEM Proceedings*. Chapman & Hall.

41. Amini, F. (2005). Potential application of paving fabrics to reduce reflective cracking. No. FHWA/MS-DOT-RD-05-174, FHWA, U.S. Department of Transportation.

42. De Bondt A. (2000). Effect of reinforcement properties. In *4th International RILEM Conference on Reflective Cracking in Pavements*, pp. 13–22.

43. Ameri, M., Mansourian, A., Khavas, M.H., Aliha, M.R.M., and M.R. Ayatollahi (2011). Cracked asphalt pavement under traffic loading–A 3D finite element analysis. *Engineering Fracture Mechanics,* Vol. 78(8), pp. 1817-1826.

44. Wang, H. and I.L. Al-Qadi (2009). Combined effect of moving wheel loading and three-dimensional contact stresses on perpetual pavement responses. *Transportation Research Record: Journal of the Transportation Research Board*, Vol. 2095(1), pp. 53–61.

45. Dehnad, M.H., Khodaii, A. and F.M. Nejad (2013). Moisture sensitivity of asphalt mixtures under different load frequencies and temperatures. *Construction and Building Materials*, Vol. 48, pp. 700-707.

46. Li, D., Rose, J., and J. LoPresti (2001). Test of hot-mix asphalt trackbed over soft subgrade under heavy axle loads. *Technology Digest-01-009*, Associations of American Railroads.

47. Al-Qadi, I.L. and W.N. Nassar (2003). Fatigue shift factors to predict HMA performance. *International Journal of Pavement Engineering*, Vol. 4(2), pp. 69-76.

48. Immanuel, S. and D.H. Timm (2006). Measured and theoretical pressures in base and subgrade layers under dynamic truck loading. In *Airfield and Highway Pavement: Meeting Today's Challenges with Emerging Technologies*, pp. 155-166.

49. Millien A., Dragomir M.L., Wendling L., Petit C., and M. Iliescu (2012). Geogrid interlayer performance in pavements: tensile-bending test for crack propagation. In *7th RILEM International Conference on Cracking in Pavements*, Vol. 2, pp. 1209–18.

50. Dave, E.V. and W.G. Buttlar (2010). Thermal reflective cracking of asphalt concrete overlays. *International Journal of Pavement Engineering*, Vol. 11(6), pp. 477-488.

51. Ceylan, H., Gopalakrishnan, K. and R.L. Lytton (2010). Neural networks modeling of stress growth in asphalt overlays due to load and thermal effects during reflection cracking. *Journal of Materials in Civil Engineering*, Vol. 23(3), pp. 221-229.

52. Al-Qadi, I.L., Hassan, M.M., and M.A. Elseifi (2005). Field and theoretical evaluation of thermal fatigue cracking in flexible pavements. *Transportation Research Record: Journal of the Transportation Research Board*, Vol. 1919(1), pp. 87–95.

53. Dave, E.V., Song, S.H., Buttlar, W.G. and G.H. Paulino (2007). Reflective and thermal cracking modeling of asphalt concrete overlays. *Advanced Testing and Characterization of Bituminous Materials*, Vol. 2, pp.1241-1252.

54. Yin, H.M., Buttlar, W.G., and G.H. Paulino, G.H (2007). Simplified solution for periodic thermal discontinuities in asphalt overlays bonded to rigid pavements. *Journal of Transportation Engineering*, Vol. 133(1), pp. 39-46.

55. Canestrari, F., Stimilli, A., Bahia, H.U., and A. Virgili (2015). Pseudo-variables method to calculate HMA relaxation modulus through low-temperature induced stress and strain. *Materials & Design*, Vol. 76, pp.141-149.

56. Kim, S.S., Wargo, A., and D. Powers (2010). Asphalt concrete cracking device to evaluate low temperature performance of HMA. *Journal of the Association of Asphalt Paving Technologists*, Vol. 79.

57. Livneh M., Ishai I., and O. Kief (1993). Bituminous pre-coated geotextile felts for retarding reflection cracks. In *RILEM Proceedings*, pp. 343–350. Chapman & Hall.

58. Gibney A., Lohan G., and C. Moore (2002). Laboratory study of resistance of bituminous overlays to reflective cracking. *Transportation Research Record: Journal of the Transportation Research Board*, Vol. 1809, pp. 184-190.

59. Ogundipe O.M., Thom N., and A. Collop (2013). Investigation of crack resistance potential of stress absorbing membrane interlayers (SAMIs) under traffic loading. *Constrution Building Materials*, Vol. 38, pp. 658–66.

60. Denolf K., De Visscher J., and A. Vanelstraete (2012). Performance of anti-cracking interface systems on overlaid cement concrete slabs-development of laboratory test to simulate slab rocking. In *7th RILEM International Conference on Cracking in Pavements*, Vol. 2, pp. 1169–80.

61. Francken L, Vanelstraete A. On the thermorheological properties of interface systems. *RILEM Proceedings*, pp. 206-219. Chapman & Hall.

62. Di Benedetto H., Neji J., Antoine J., and M. Pasquier (1993). Apparatus for laboratory study of cracking resistance. In: Proceedings of the 2nd international RILEM conference on reflective cracking in pavements; 1993. p. 179–86.

63. Dempsey, B. (2002). Development and performance of interlayer stress-absorbing composite in asphalt concrete overlays. *Transportation Research Record: Journal of the Transportation Research Board*, Vol. 1809, pp. 75–83.

64. Zhou F. and T. Scullion (2005). Overlay tester: a rapid performance related crack resistance test. Public FHWA/TX-05/0-4467-2, FHWA, U.S. Department of Transportation.

65. Sousa J.B., Shatnawi S., and J. Cox (1996). An approach for investigating reflective fatigue cracking in asphalt-aggregate overlays. In *RILEM Proceedings*, pp. 103-112. Chapman & Hall.

66. Dumas P. and J. Vecoven (1993). Processes reducing reflective cracking: synthesis of laboratory tests. In *RILEM Proceedings*, pp. 246–53. Chapman & Hall.

67. Prieto J., Gallego J., and I. Pérez (2007). Application of the wheel reflective cracking test for assessing geosynthetics in anti-reflection pavement cracking systems. *Geosynthetics International*, Vol. 14(5), pp. 287–97.

68. Moreno-Navarro F. and M.C. Rubio-Gámez (2013). UGR-FACT test for the study of fatigue cracking in bituminous mixes. *Constrution Building Materials*, Vol. 43, pp. 184–90.

69. Moreno-Navarro, F., Sol-Sanchez, M., and M.C. Rubio-Gamez (2014). Reuse of deconstructed tires as anti-reflective cracking mat systems in asphalt pavements. *Construction and Building Materials*, pp. 182-189.

70. Sobhan K., Crooks T., Tandon V., and S. Mattingly (2004). Laboratory simulation of the growth and propagation of reflection cracks in geogrid reinforced asphalt overlays. In *Proceedings of the 5th International RILEM Conference on Cracking in Pavements*, pp. 589–96.

71. Gonzalez-Torre, I., Calzada-Perez, M.A., Vega-Zamanillo, A. and D. Castro-Fresno (2015). Evaluation of reflective cracking in pavements using a new procedure that combine loads with different frequencies. *Construction and Building Materials*, Vol. 75, pp. 368-374.

72. Morian, A.D., Zhao, Y., Arrelano, J., and E.D. Hall (2005). Analysis of asphalt pavement rehabilitation treatment performance over twenty years. *Transportation Research Record: Journal of the Transportation Research Board*, Vol. 1905, pp. 36-43.

73. Greene, J., Choubane, B., Chun, S., and S. Kim (2012). *Effect of asphalt rubber membrane interlayer (ARMI) on instability rutting and reflection cracking of asphalt mixture*. Report No. FL/DOT/SMO/12-552, Florida Department of Transportation.

74. Li, V.C., Wang, S. and Wu, C. (2001). Tensile strain-hardening behavior of polyvinyl alcohol engineered cementitious composite (PVA-ECC). ACI Materials Journal-American Concrete Institute, 98(6), pp.483-492.

75. Marzougui, D., Buyuk, M., and S. Kan (2007). Performance evaluation of portable concrete barriers. No. DTFH61-02-X-0007, NCAC Report 4.

76. Li, V.C., Mishara, D.K., Naaman, A.E., Wight, J.K., LaFave, J.M., Wu, H.C., and Y Ianada (1994). On the shear behavior of engineered cementitious composites. *Advanced Cement Based Materials*, Vol. 1(3), pp. 142-149.

77. Li, V.C., Fukuyama, H., and A. Mikame (1998). Development of ductile engineered cementitious composite elements for seismic structural applications. In *Proceedings of Structural Engineering World Congress (SEWC)*, Paper T177-5, San Francisco, CA.

78. Li, V.C. (2003). On engineered cementitious composites (ECC). *Journal of Advanced Concrete Technology*, pp. 215-230.

79. Li, V.C. (2008). Engineered cementitious composites (ECC) material, structural, and durability performance.

80. Maalej, M. and V.C. Li (1995). Introduction to strain-hardening engineered cementitious composites in design of reinforced concrete flexural members for improved durability. *ACI Structural Journal*, Vol. 92(2), pp. 167-176.

81. Bentur, A. and S. Mindess (1990). Fiber-reinforced cementitious composites. Elsevier Applied Science. *London and New York*.

82. Zhang, H., Keoleian, G.A., and M.D. Lepech (2008). An integrated life cycle assessment and life cycle analysis model for pavement overlay systems. In *Proceedings of the 1st International Symposium on Life-Cycle Civil Engineering*, pp. 907-915. London: Taylor & Francis Group.

83. Wang, S. and V.C. Li (2007). Engineered cementitious composites with high-volume fly ash. *ACI Materials Journal*, Vol. 104(3), pp. 233–241.

84. Yang, E.-H., Garces, E.O., and V.C. Li (2013). Micromechanics-based optimization of pigmentable strain-hardening cementitious composites. *Journal of Materials in Civil Engineering*, Vol. 26(7), 04014017.

85. Wang, S. (2005). *Micromechanics based matrix design for engineered cementitious composites*. PhD Thesis, University of Michigan.

86. Yang, E.-H., Yang, Y., and V.C. Li (2007). Use of high volumes of fly ash to improve ECC mechanical properties and material greenness. *ACI Materials Journal,* Vol. 104(6), pp. 620–628.

87. Yang, E. and V.C. Li (2006). Rate dependence in engineered cementitious composites. In *International RILEM Workshop on High Performance Fiber Reinforced Cementitious Composites in Structural Applications*, pp. 83–92.

88. Zhang, M.-H. (1995). Microstructure, crack propagation, and mechanical properties of cement pastes containing high volumes of fly ashes. *Cement and Concrete Research*, Vol. 25(6), pp. 1165–1178.

89. Şahmaran, M., Yaman, Ö., and M. Tokyay (2007). Development of high-volume low-lime and high-lime fly-ash-incorporated self-consolidating concrete. *Magazine of Concrete Research*, Vol. 59 (2), pp. 97-106.

90. Li, V.C. (2006). Bendable composites: ductile concrete for structures. *Structure Maganize*, Vol. 4548.

91. Li, V.C. (1998). Engineered cementitious composites-tailored composites through micromechanical modeling.

92. Ranade, R., Li, V.C., Stults, M.D., Heard, W.F. and T.S. Rushing (2013). Composite properties of high-strength, high-ductility concrete. *ACI Materials Journal*, Vol. 110(4).

93. Nath, F. and M. Mokhtari (2018). Optical visualization of strain development and fracture propagation in laminated rocks. *Journal of Petroleum Science and Engineering*, 354-365.

94. Pan, B., Qian, K., Xie, H. and A. Asundi (2009). Two-dimensional digital image correlation for in-plane displacement and strain measurement: A review. *Measurement Science and Technology*, 20(6), p.062001.

95. Hung, P.C. and A.S. Voloshin (2003). In-plane strain measurement by digital image correlation. *Journal of the Brazilian Society of Mechanical Sciences and Engineering*, 25(3), pp.215-221.

96. Kang, J., Ososkov, Y., Embury, J.D. and D.S. Wilkinson, D.S. (2007). Digital image correlation studies for microscopic strain distribution and damage in dual phase steels. *Scripta Materialia*, 56(11), pp.999-1002.

97. Chantachot, T., Kongkitkul, W., Youwai, S., and P. Jongpradist (2016). Behaviours of geosynthetic-reinforced asphalt pavements investigated by laboratory physical model tests on a pavement structure. *Transportation Geotechnics*, 103-118.

98. Saride, S., and V.V. Kumar (2017). Influence of geosynthetic-interlayers on the performance of asphalt overlays on pre-cracked pavements. *Geotextiles and Geomembranes*, 184-196.

99. Kumar, V.V. and S. Saride (2018). Evaluation of cracking resistance potential of geosynthetic reinforced asphalt overlays using direct tensile strength test. *Construction and Building Materials*, 37-47.

100. Gurung, N. (2003). A laboratory study on the tensile response of unbound granular base road pavement model using geosynthetics. *Geotextiles and Geomembranes*, 21(1), pp.59-68.